

## BIROn - Birkbeck Institutional Research Online

Yan, Z. and Tian, Y. and Vermeesch, P. and Sun, X. and Rittner, M. and Carter, Andrew and Shao, C. and Huang, H. and Ji, X. (2018) Late Triassic tectonic inversion in the upper Yangtze Block: insights from detrital zircon U–Pb geochronology from southwestern Sichuan Basin. *Basin Research* 31 (1), pp. 92-113. ISSN 0950-091X.

Downloaded from: <http://eprints.bbk.ac.uk/23611/>

*Usage Guidelines:*

Please refer to usage guidelines at <http://eprints.bbk.ac.uk/policies.html>  
contact [lib-eprints@bbk.ac.uk](mailto:lib-eprints@bbk.ac.uk).

or alternatively

1 **Late Triassic tectonic inversion in the upper Yangtze Block: insights from**  
2 **detrital zircon U–Pb geochronology from southwestern Sichuan Basin**

3  
4 Zhaokun Yan<sup>1,3,4</sup>, Yuntao Tian<sup>3\*</sup>, Rui Li<sup>3</sup>, Pieter Vermeesch<sup>4</sup>, Xilin Sun<sup>3</sup>, Yong Li<sup>2</sup>, Martin Rittner<sup>4</sup>,  
5 Andrew Carter<sup>6</sup>, Chongjian Shao<sup>2</sup>, Hu Huang<sup>2</sup>, Xiangtian Ji<sup>2</sup>

6  
7 <sup>1</sup> *State Key Laboratory of Mineral Deposits Research, School of Earth Sciences and Engineering,*  
8 *Nanjing University, Nanjing 210023, China*

9 <sup>2</sup> *State Key Laboratory of Oil and Gas Reservoir Geology and Exploitation (Chengdu University of*  
10 *Technology), Sichuan Chengdu, 610059, China*

11 <sup>3</sup> *Guangdong Provincial Key Lab of Geodynamics and Geohazards, School of Earth Sciences and*  
12 *Engineering, Sun Yat-sen University, Guangzhou 510275, China*

13 <sup>4</sup> *Department of Earth Sciences, University College London, London, WC1E 6BT, UK*

14 <sup>5</sup> *Cluster Geology and Geochemistry, VU University Amsterdam, De Boelelaan 1085, 1081 HV*  
15 *Amsterdam, The Netherlands*

16 <sup>6</sup> *Department of Earth and Planetary Science, Birkbeck University of London, Malet Street,*  
17 *Bloomsbury, London WC1E 7HX, UK*

18  
19  
20 \*Corresponding author:

21 Yuntao Tian

22 School of Earth Sciences and Engineering

23 Sun Yat-sen University

24 Guangzhou, China

25 Email: tianyuntao@mail.sysu.edu.cn

26  
27  
28 **ABSTRACT**

29 The Sichuan Basin and the Songpan-Ganze terrane, separated by the Longmen Shan fold-and-thrust  
30 belt (the eastern margin of the Tibetan Plateau), are two main Triassic depositional centers, south of the  
31 Qinling-Dabie orogen. During the Middle – Late Triassic closure of the Paleo-Tethys Ocean the  
32 Sichuan Basin region, located at the western margin of the Yangtze Block, transitioned from a passive  
33 continental margin into a foreland basin. In the meantime, the Songpan-Granze terrane evolved from a  
34 marine turbidite basin into a fold-and-thrust belt. To understand if and how the regional sediment  
35 routing system adjusted to these tectonic changes, we monitored sediment provenance primarily by  
36 using detrital zircon U-Pb analyses of representative stratigraphic samples from the southwestern edge  
37 of the Sichuan Basin. Integration of the results with paleocurrent and published detrital zircon data  
38 from other parts of the basin identified a marked change in provenance. Early-Middle Triassic samples  
39 were dominated by Neoproterozoic (~700-900Ma) zircons sourced mainly from the northern Kangdian  
40 basement, whereas Late Triassic sandstones recorded a more diverse range of zircon ages, sourced  
41 from the Qinling, Longmen Shan and Songpan-Ganze terrane. This change reflects a major drainage  
42 adjustment in response to the Late Triassic closure of the Paleo-Tethys Ocean and significant

43 shortening in the Longmen Shan thrust belt and the eastern Songpan-Ganze terrane. Further, by Late  
44 Triassic time, the uplifted northern Kangdian basement had subsided. Considering the eastward  
45 paleocurrent and depocenter geometry of the Upper Triassic deposits, subsidence of the northern  
46 Kangdian basement probably resulted from eastward shortening and loading of the Songpan-Ganze  
47 terrane over the western margin of the Yangtze Block in response to the Late Triassic collision between  
48 Yangtze Block, Yidun arc and Qiangtang terrane along the Ganze-Litang and Jinshajiang sutures.  
49  
50

## 51 INTRODUCTION

52 The Sichuan Basin, located along the western margin of the Yangtze Block, shares common  
53 borders with five major tectonic terrains: (1) Qinling-Dabie orogen to the north, (2) the Songpan-Ganze  
54 terrane (i.e. the eastern Tibetan Plateau) to the northwest, (3) the Yidun arc to the west, (4) Kangdian  
55 Basement to the south and (5) the eastern Sichuan fold-and-thrust belt to the east (Fig. 1). Numerous  
56 structural, geochronological, and sedimentary studies suggested that these areas had experienced a  
57 significant phase of crustal shortening and rock exhumation during Triassic closure of the Paleo-Tethys  
58 Ocean (Burchfiel *et al.*, 1995; Zhang *et al.*, 1995; Yin, 1996; Meng & Zhang, 2000; Li *et al.*, 2003a;  
59 Wang *et al.*, 2005; Jia *et al.*, 2006), and that tectonic loading over the margins Sichuan Basin changed  
60 the setting from a passive continental margin to a foreland basin.

61 In the context of these changes, the provenance of sediments deposited in the Sichuan Basin have  
62 seen extensive study, much based on detrital zircon U-Pb geochronology (Deng *et al.*, 2008; Chen,  
63 2011; Luo *et al.*, 2014; Zhang *et al.*, 2015a; Li *et al.*, 2016; Shao *et al.*, 2016; Zhu *et al.*, 2017). Results  
64 from previous work suggest that sediments in the basin were mainly sourced from the Qinling-Dabie  
65 orogen, to the north, and the Longmen Shan thrust belt and the Songpan-Ganze terrane to the west.  
66 However, most of those previous studies focused on the Late Triassic - Cretaceous foreland basin  
67 sediments in the western and northern part of the Sichuan Basin (Fig. 1). The provenance of Early and  
68 Middle Triassic passive continental margin deposits is unknown. Constraining the provenance of  
69 sediments deposited before and after Late Triassic inversion of the Sichuan Basin could provide  
70 significant insights into whether the sediment routing system into the basin had significantly changed.

71 Previous sedimentary and stratigraphic studies showed that the Early – Middle Triassic  
72 paleogeography is characterized by a lateral facies transition from clastic to carbonate away from the  
73 southern edge of the basin to the interior (Liu & Tong, 2001; Long *et al.*, 2011; Zhao *et al.*, 2012; Tan  
74 *et al.*, 2014; Wei *et al.*, 2014), indicating that the southwestern basin margin was bounded and sourced  
75 by a highland to the south. The highland consists of Neoproterozoic basement and is referred to as the  
76 Kangdian basement (referred to the Kangdian Oldland or Kangdian Axis by Chinese researchers) (Li,  
77 1963; Luo, 1983; Wang *et al.*, 1983; Dai *et al.*, 2012; Tan *et al.*, 2013) (Fig. 1). However, in response  
78 to closure of the Paleo-Tethys Ocean, the entire basin transitioned into a foreland basin with detritus  
79 sourced mainly from the Longmen Shan thrust belt and the Qinling-Dabie orogen to the west and north  
80 of the basin. These earlier sedimentary studies imply a significant change in sediment provenance  
81 during Late Triassic basin inversion. To test this we applied detrital zircon geochronology to a series of  
82 Early-Late Triassic sandstone samples collected from the southwestern part of the Sichuan Basin.  
83 Depositional ages of sampled rocks are constrained by new zircon U-Pb results derived from a newly  
84 mapped volcanic tuff. The results are interpreted together with previously mapped stratigraphic

85 correlations and paleocurrent data, in order to constrain the paleogeographic evolution of the  
86 southwestern margin of the Sichuan Basin during Early-Late Triassic time, and to test if and how  
87 crustal shortening and rock uplift during the Triassic had influenced sedimentary routing network  
88 across the basin margin.  
89

## 90 **GEOLOGICAL SETTING**

91 The southwestern part of the Sichuan Basin is bounded by the Kangdian basement uplift to the  
92 south and the Songpan-Ganze terrane and Longmen Shan to the west (Figs 1, 2). The Triassic and  
93 Cenozoic geological evolution of these major terranes is summarized below.

### 94 **Regional Tectonism**

95 Triassic evolution of the Sichuan Basin and surrounding regions was controlled by the  
96 Middle - Late Triassic closure of the Paleo-Tethys Ocean along the Mianlue suture, forming the  
97 Qinling-Dabie orogen (e.g. Zhang, *et al.*, 1995; Yin, 1996; Meng, & Zhang, 2000; Li, *et al.*, 2003a),  
98 and the Litang and Jinshajiang sutures north and south of the Yidun arc (Fig. 1, e.g. Reid *et al.*,  
99 2005; Roger *et al.*, 2008; Pullen *et al.*, 2008; Roger *et al.*, 2010; Yuan *et al.*, 2010; Wang *et al.*,  
100 2013a). During this time basin margins, especially the Longmen Shan and Songpan-Ganze  
101 turbidite terrane to the west, were significantly shortened (e.g. Huang *et al.*, 2003; Yan *et al.*, 2011;  
102 Weller *et al.*, 2013; Zheng *et al.*, 2016), inducing several kilometers of flexural subsidence (e.g. Guo  
103 *et al.*, 1996; Li, *et al.*, 2003a; Meng *et al.*, 2005). By the Cenozoic basin margins were reactivated  
104 by the Indo-Asian collision and the subsequent outward growth of the Tibetan Plateau  
105 (Enkelmann *et al.*, 2006; Liu-Zeng *et al.*, 2008; Wang *et al.*, 2012a; Tian *et al.*, 2012, 2013).

### 106 **Sichuan Basin**

107 Phanerozoic evolution of the Sichuan Basin can be divided into three major stages: a passive  
108 margin stage characterized by platform carbonates during Paleozoic to Middle Triassic time (Xu *et al.*,  
109 1997), a Late Triassic foreland basin characterized predominantly by continental siliciclastic  
110 sedimentation (Li *et al.*, 2003a), and a prolonged phase of denudation in the eastern and central  
111 Sichuan Basin since the Late Cretaceous, as shown by thermochronological studies (Tian *et al.*, 2012;  
112 Yang *et al.*, 2017). In this study, we focus on the provenance of the Triassic detritus in the southwest  
113 Sichuan Basin that consists of, from bottom to top, the Feixianguan, Jialingjiang, Leikoupo, Maantang,  
114 Xiaotangzi and Xujiuhe Formations, (Fig. 3).

115 (1) The marine Feixianguan Formation is widely distributed in the Sichuan Basin and shows  
116 marked lateral lithofacies variations. The formation consists of purple shale and sandy shale,  
117 interbedded with grey limestone, oolitic limestone, marl and sandstone in western parts of the basin,  
118 which changes into limestone toward the eastern basin (BGMRS, 1997). The biostratigraphic age of  
119 the formation is earliest Triassic (BGMRS, 1997), ~252 Ma supported by zircon U-Pb ages from  
120 volcanic ash beds at the bottom of the formation (Burgess *et al.*, 2014). The isopach map of this  
121 formation shows a depocenter located in the center of the basin (Fig. 4c).

122 (2) The marine Jialingjiang Formation conformably overlies the Feixianguan Formation, and is  
123 mainly composed of limestone and dolomite (BGMRS, 1997). In the formation, Late-Early Triassic

124 bivalves, ammonites, foraminiferas and conodonts have been discovered (BGMRSP, 1997). The top of  
125 the formation is marked by a widespread thin layer (the thickness is 10s cm – 1 m) of altered tuff  
126 (named as “green-bean rocks” in early Chinese literature) (Zhu & Wang, 1986), that has been dated as  
127 ~247 Ma by ID-TIMS, LA-ICP-MS and CA-TIMS on zircon (Ovtcharova *et al.*, 2006; Xie *et al.*, 2013;  
128 Lehrmann *et al.*, 2015).

129 (3) The marine Leikoupo Formation mainly consists of dolomite and argillaceous dolomite,  
130 interbedded with limestone and gypsum layers (BGMRSP, 1997). It contains Middle Triassic bivalves  
131 and ammonites such as *Progonoceratites*, *Beyrichites* (BGMRSP, 1997). The boundary between the  
132 Leikoupo and underlying Jialingjiang Formations is marked by an altered tuff. The isopach map of this  
133 formation shows a depocenter located in the center of the Sichuan Basin (Fig. 4b).

134 (4) The marine Maantang Formation, distributed in the western Sichuan Basin, mainly consists of  
135 marine black mudstone and shale interbedded with siltstone, marl, oolitic and bioclastic limestones and  
136 sponge reefs (BGMRSP, 1997; Li *et al.*, 2003a). It is regarded as Carnian in age on the basis of its  
137 fossil content (Shi *et al.*, 2016). The Kuahongdong Formation represents equivalent coeval strata along  
138 the southwestern margin of the basin, and is composed of conglomerate, mudstone, argillaceous  
139 limestone and argillaceous dolomite (BGMRSP, 1997).

140 (5) The Xiaotangzi Formation, is composed of black marine shale, mudstone, quartz arenite, lithic  
141 arenite and siltstone, and can be divided into three parts: a lower part composed of black shale  
142 interbedded with quartz arenite, a middle part composed of lithic arenite and black shale, and an upper  
143 part composed of arkose. The formation coarsens upwards and is thought to represent a transition from  
144 marine shelf to delta environments. It has an early Norian age based on its fossil content (Li *et al.*,  
145 2003a).

146 (6) The Xujiahe Formation conformably overlies the Xiaotangzi Formation in the western  
147 Sichuan Basin, and unconformably overlies Middle Triassic limestone of the Leikoupo Formation in  
148 the central and eastern Sichuan Basin. Widely distributed, the lithology and facies of this formation  
149 changes from coarse-grained sediments, including alluvial conglomerates along the front of the  
150 Longmen Shan thrust belt, to fine-grained lacustrine deposits in the basin interior. Two depocenters  
151 developed, one in front of the central segment of the Longmen Shan thrust belt and the other in areas to  
152 the south (Fig. 4a). Depositional age of the formation is late Norian to Rhaetian based on the fossil  
153 content (WGCMSPISB, 1984; Li *et al.*, 2003a).

154 Previous sedimentary studies suggested that the clastic deposits of the Feixianguan, Jialingjiang  
155 and Leikoupo Formations in the southwestern margin of the Sichuan Basin were sourced from the  
156 south, as shown by a facies transition from clastic to carbonate deposits from the margin to the interior  
157 of the basin (Feng *et al.*, 1997; Tan *et al.*, 2014; Sun *et al.*, 2015). The Kangdian basement might be the  
158 source of Upper Triassic sediments, as suggested by studies on the detrital mineral assemblage,  
159 sedimentary system and conglomerate composition (Xie *et al.*, 2006; Jiang *et al.*, 2007; Shi *et al.*,  
160 2010). However, nonmarine Late Triassic sediments unconformably overlie the Kangdian basement  
161 (BGMRSP, 1991) indicating that the region was likely an area of deposition rather than erosion (Liu &  
162 Tong, 2001; Wei *et al.*, 2014).

## 163 **Kangdian Basement**

164 The Kangdian basement forms the western margin of the Yangtze Block and extends for over 700  
165 km from the city of Kangding in the north to the city of Yuanmou in the south (Zhou *et al.*, 2002; Zhu  
166 *et al.*, 2011). It is located on the western margin of the Yangtze Block (Fig. 1), and mainly consists of

167 Neoproterozoic basement, overlain by marine Paleozoic cover and locally by Late Triassic to Cenozoic  
168 terrestrial sediments (BGMRSP, 1991). The U-Pb age of basement has been dated as ~740–870 Ma (Li  
169 *et al.*, 2003b; Zhao & Zhou, 2007; Sun *et al.*, 2009).

170 There is a debate on the Paleozoic and Mesozoic paleogeography of Kangdian area. One model  
171 depicts the Kangdian area as a region of erosion between the Ordovician and Carboniferous (Li, 1963),  
172 followed by a rift subsidence stage from Late Permian to Jurassic (Luo, 1983; Guo *et al.*, 1996).  
173 Alternately, the Paleozoic - Mesozoic geological evolution of the region can be divided into three  
174 stages: a stable marine platform from the Cambrian to Early Permian, an uplift stage affected by  
175 Emeishan mantle plume from Late Permian to Middle Triassic, and transtensional subsidence during  
176 the Late Triassic and Jurassic (Chen *et al.*, 1987; Feng *et al.*, 1994; Wang *et al.*, 1994; He *et al.*, 2003;  
177 Chen *et al.*, 2011).

### 178 Longmen Shan thrust belt

179 The Longmen Shan is approximately >500km long and 30 - 50km wide, and defines the eastern  
180 margin of the Tibetan Plateau. It separates the strongly folded and faulted Songpan-Ganze terrane to  
181 the west from weakly deformed Sichuan Basin rocks to the east (Fig. 1). Outcrops in the Longmen  
182 Shan are mostly Neoproterozoic basement and overlying Paleozoic sedimentary strata. Zircon U-Pb  
183 analyses of Neoproterozoic basement rocks yielded ages mainly between 770-890 Ma (Fu *et al.*, 2013),  
184 comparable to the age of Kangdian basement rocks, which also share similar petrology.

185 The Longmen Shan thrust belt experienced three phases of crustal shortening in the Early  
186 Mesozoic and Late Cenozoic. Various lines of geochronological and structural evidence have been  
187 reported for the Late Triassic formation of the Longmen Shan thrust belt (Huang *et al.*, 2003; Yan *et al.*,  
188 2011; Weller *et al.*, 2013), including (i) Late Triassic Barrovian metamorphism recorded by monazite  
189 U–Th–Pb and garnet Sm–Nd ages (204-190 Ma), derived from metamorphosed rocks in the Danba  
190 Antiform, immediately south of the Longmen Shan (Huang *et al.*, 2003; Weller *et al.*, 2013), (ii)  
191 Mid-Late Triassic shortening (237-208 Ma) as dated by muscovite  $^{40}\text{Ar}/^{39}\text{Ar}$  ages of early Paleozoic  
192 schistose rocks from the northern Longmen Shan (Yan *et al.*, 2011), and (iii) Late Triassic formation of  
193 the foreland basin system in the Sichuan Basin (Guo *et al.*, 1996; Li *et al.*, 2003). The second phase of  
194 Late Cretaceous – Early Paleogene deformation is characterized by contemporaneous hinterland-ward  
195 shearing and foreland-ward thrusting at the back and front sides of the Longmen Shan thrust belt, based  
196 on structural mapping and synkinematic mica  $^{40}\text{Ar}/^{39}\text{Ar}$  geochronological analyses (Tian *et al.*, 2016).  
197 The last phase of deformation occurred in the Late Cenozoic, during which pre-existing structures were  
198 reactivated by the eastward growth of the Tibetan Plateau (e.g. Wang *et al.*, 2012a; Tian *et al.*, 2013).

### 199 Songpan-Ganze terrane

200 The Songpan-Ganze terrane currently forms a triangular fold belt wedged between the North  
201 China Block, Yangtze Block, and Qaidam Block (Fig. 1). More than 80% of the Songpan-Ganze  
202 terrane is covered by thick Triassic turbidites, which were mainly sourced from the Qinling-Dabie  
203 orogen to the northeast and terranes to the north (Enkelmann *et al.*, 2007; Weislogel *et al.*, 2010; Ding  
204 *et al.*, 2013). By latest Triassic, the Songpan - Ganze basin had shallowed, recorded by coeval  
205 coal-bearing clastic deposits (BGMRSP, 1991; Chang, 2000). In response to closure of the  
206 paleo-Tethys Ocean the flysch basin evolved into a fold belt during Late Triassic time (Xu *et al.*, 1992;  
207 Roger *et al.*, 2011). Jurassic – Cenozoic deposits, have been recently reported in the western part of the

208 terrane (Ding *et al.*, 2013).

209 The Songpan-Ganze terrane was intruded by Late Triassic–Jurassic granitoids (Roger *et al.*, 2011),  
210 with emplacement ages in the range 228 - 153 Ma (Roger, *et al.*, 2004; Zhang, *et al.*, 2006; Xiao, *et al.*,  
211 2007; Zhang, *et al.*, 2007; Weislogel, 2008; Yuan, *et al.*, 2010). Metamorphic overprinting is relatively  
212 strong along the terrane margins where mudstones were metamorphosed to phyllite, but weak within  
213 the basin interior (Chang, 2000).

214

## 215 PREVIOUS DETRITAL ZIRCON STUDIES

216 Over the past decade, the provenance of the Late Triassic clastic sediments in the Sichuan Basin  
217 has been intensively studied, especially by detrital zircon geochronology (Fig. 1), but this has led to  
218 conflicting conclusions. Deng *et al.* (2008) reported ages of four Late Triassic sandstone samples from  
219 the western Sichuan Basin and the eastern Songpan-Ganze terrane, and suggested that the Late Triassic  
220 Xujiahe Formation was sourced from the Songpan-Ganze terrane and Longmen Shan thrust belt. By  
221 contrast the study of Chen (2011) based in the northern and western parts of the Sichuan Basin  
222 indicated that the Qinling orogen to the north was the main source of sediments. Recently work by Luo  
223 *et al.* (2014), Zhang *et al.* (2015a) and Shao *et al.* (2016), suggest that the Longmen Shan thrust belt  
224 and the Songpan-Ganze terrane in the west and the Qinling-Dabie orogen in the north were the source  
225 of the Late Triassic sediments in the western and northern Sichuan Basin, respectively. Zhang *et al.*  
226 (2015a) and Shao *et al.* (2016) also indicated the minor role of the north Yangtze Block in supplying  
227 sediments to the northern Sichuan Basin. Shao *et al.* (2016) suggested that sediments of the western,  
228 southern and eastern parts of basin shared the same sources that include the Qinling orogen, southern  
229 North China Block, the eastern Songpan-Ganze terrane and the Longmen Shan thrust belt. Zhu *et al.*  
230 (2017) reported detrital zircon ages of four Middle-Late Triassic sandstone samples from the  
231 southwestern Sichuan Basin, and suggested that Middle Triassic sediments mainly sourced from the  
232 Kangdian basement and Emeishan Large Igneous Province to the south, whereas Late Triassic  
233 sediments came mainly from the Songpan-Ganze terrane and Yidun arc to the west with a minor  
234 component from the Qinling orogen to the north and Jiangnan Xuefeng thrust belt (southeastern  
235 Yangtze Block) to the east. Importantly, most of these previous studies focused on the Late Triassic;  
236 little is known about the source of the Early Triassic clastic rocks. A core aim of this study therefore, is  
237 to try and resolve the ongoing debate about the sources of the Triassic sediments.

## 238 SAMPLING AND ANALYTICAL METHODS

239 Samples were collected from the Longcanggou, Longmendong and Chuanzhu sections in the  
240 southwestern part of the Sichuan Basin. These sections expose all Triassic formations (Figs 5 and 6).  
241 Details of the stratigraphy and sedimentology for each sections is provided in the supplementary text.  
242 Samples include two sandstones from the Early Triassic Feixianguan (T<sub>1f</sub>) and Jialingjiang Formation  
243 (T<sub>1j</sub>), one volcanic tuff sample from the boundary between the Jialingjiang Formation (T<sub>1j</sub>) and  
244 Leikoupo (T<sub>2l</sub>), two sandstones from the Middle Triassic Leikoupo Formation (T<sub>2l</sub>) and five sandstones  
245 from the Upper Triassic Maantang (T<sub>3m</sub>) Xiaotangzi (T<sub>3xt</sub>) and Xujiahe Formations (T<sub>3x</sub>) (Figs 5 and  
246 6).

247 Paleocurrent measurements were made based on cross-bedding and ripples in sandstone beds. The  
248 orientations of trough cross laminations were measured using the method described by DeCelles *et al.*

249 (1983). Eighteen sandstones with no evident diagenetic alteration were selected from three  
250 sections (Fig. 6) and were point counted using photomicrographs following the Gazzi-Dickinson  
251 method (Dickinson et al., 1983). The statistics are presented in supplementary tables 1.

252 Ten samples were selected for detrital zircon U-Pb analysis. Analyses were made by LA-ICP-MS  
253 using the facilities at the London Geochronology Centre, University College London, based on a New  
254 Wave NWR193 excimer laser ablation system and an Agilent 7700x quadrupole mass spectrometer.  
255 The laser was set to produce  $\sim 2.5 \text{ J/cm}^2$  energy density at 8 Hz repetition rate for 25 seconds. The spot  
256 diameter was set to 25  $\mu\text{m}$  for all analyses. Repeated measurements of internal U/Pb age standard  
257 Plešovice [TIMS reference age of  $337.13 \pm 0.37 \text{ Ma}$  (Sláma et al., 2008)] and NIST-610 silicate glass  
258 (Jochum et al., 2011) were used to correct for instrumental mass bias and laser-pit-depth-dependent  
259 isotopic fractionation. GJ-1 (Jackson et al., 2004) and 91500 zircon (Wiedenbeck et al., 2004) were  
260 used as external standards. In general 100 or more single grain ages were collected for each sample.  
261 Data reduction was processed using the GLITTER software package (Griffin et al., 2008).

## 262 RESULTS

### 263 Paleocurrent

264 Paleocurrent data were collected from 7 sites, as summarized in the Fig. 2. The paleocurrent in the  
265 Feixianguan Formation, measured in the Longcanggou section (L01), is eastward (Fig. 5). The results,  
266 derived from cross-bedding and current ripples in sandstone in the Longcanggou (L02), Chuanzhu  
267 (C01, C02) and Hanyuan areas (YD01, SQ02, HY01), indicates an eastward and southeastward  
268 paleocurrent direction for the Xiaotangzi and Xujiahe Formations (Fig. 5).  
269

### 270 Sandstone petrology

271 The Early Triassic sandstones are texturally immature, with poor sorting sand (Fig. 5).  
272 Sandstones from Early Triassic Feixianguan and Jialingjiang Formation (Fig.6) are  
273 quartzo-feldspatho-litho to feldspatho-quartzose-litho sedimentaastic (classification after  
274 Garzanti (2016) ) (Figure 5f). Seven samples from the Longcanggou and Longmendong sections  
275 yield an average composition QFL = 23:25:52 (Fig. 7a). Quartz grains are generally  
276 monocrystalline and subangular to subrounded (Figure 5f). Feldspars range from 19% to 30% and  
277 are altered. Lithic fragment compositions are 30% metamorphic, 32% volcanic and 38%  
278 sedimentary (Fig. 7b). Volcanic grains are mainly basaltic debris.

279 Sandstones from the Middle Triassic Leikoupo Formation are feldspatho-litho-quartzose to  
280 litho-feldspatho-quartzose (average composition QFL = 81:8:11, LmLvLs = 29:17:51) (Figs. 5g,  
281 7a). Quartz grains are mainly monocrystalline (74%) with considerably polycrystalline (7%).  
282 Lithic fragments are mainly siltstone, with minor chert, quartzite, schist, and basaltic debris.

283 Sandstones from the Late Triassic (Fig. 6) are mainly litho-quartzose (average composition  
284 QFL = 74:7:19, LmLvLs = 27:9:64) (Figs. 5h, 5i, 5j, 7). Quartz grains are mainly monocrystalline  
285 (69%) with considerably polycrystalline (5%). Lithic fragments are mainly siltstone and slate,  
286 with minor chert, limestone, quartzite, schist, and volcanic.  
287



## 288 Zircon U-Pb isotopic results

289 In total, 1132 detrital zircons from nine detrital samples were analyzed. The U-Pb data for each  
290 sample are presented in [supplementary tables 2-3](#). As with convention, we only consider U-Pb ages that  
291 were no more than 15% discordant or 5% reverse discordant (e.g., Rittner et al., 2016). The age  
292 distributions are displayed as kernel density estimate (KDE, [Vermeesch, 2012](#)) plots.

### 293 *Altered tuff*

294 Sample SZ02 (102°51'42.92" E, 29°40'47.12"N) of the altered tuff was collected from the  
295 boundary between the Leikoupo and the underlying Jialingjiang Formations in the Longcanggou  
296 section. Some 30 out of 34 analyses yielded concordant ages most of which define a weighted mean  
297  $^{206}\text{Pb}/^{238}\text{Pb}$  age of  $246.5 \pm 1.7$  Ma ( $n=26$ ) ([Fig. 8](#)), which is similar to previous studies at other sites of  
298 the Yangtze Block, hundreds of kilometers away from our study area ([Ovtcharova et al., 2006](#); [Xie et](#)  
299 [al., 2013](#); [Lehrmann et al., 2015](#)). This new result provides an independent age constraint for  
300 deposition of the Triassic strata studied in this work. The raw data and calculated dates are presented in  
301 [supplementary Table 2](#).

### 302 *Early Triassic Feixianguan and Jialingjiang Formations*

303 Sample LCG01 (102°51'42.92" E, 29°40'47.12"N), a grey-green fine-grained sandstone, was  
304 collected from the Feixianguan Formation in the Longcanggou section ([Fig. 6](#)). Ninety-nine of 156  
305 analyses yielded concordant ages, which range from ca.  $243 \pm 3$  Ma to 2.4 Ga. The KDE plot of this  
306 sample shows a major peak at  $\sim 800$  Ma (34%), and three minor peaks at  $\sim 248$  Ma (8%),  $\sim 510$  Ma  
307 (14%) and  $\sim 950$  Ma (19%) ([Fig. 9a](#)).

308 Sample LMD02 (103°25'5.73" E, 29°34'46.76"N), a grey-purple coarse sandstone, was collected  
309 from the Jialingjiang Formation in the Longmendong section ([Fig. 6](#)). Of 129 analyses, 123 yielded  
310 concordant ages. Nearly all ages are between 730 - 880 Ma, showing a dominant peak at  $\sim 800$  Ma in  
311 the KDE plot ([Fig. 9b](#)).

### 312 *Middle Triassic Leikoupo Formation*

313 Two samples (grey coarse-grained sandstone), LCG03 (102°51'35.19" E, 29°40'51.35"N) and  
314 LCG04 (102°51'35.05" E, 29°40'51.18"N), were collected from the Leikoupo Formation exposed at the  
315 Longcanggou section ([Fig. 6](#)). One hundred and thirty-six out of the 153 zircon grains analysed gave  
316 concordant ages that ranged from ca.  $242 \pm 3$  Ma to 2.5 Ga, with 74% lying between 730 Ma and 880  
317 Ma, showing a dominant mode at  $\sim 800$  Ma ([Fig. 9c](#)), similar to the lower sample LMD02 from the  
318 Jialingjiang Formation.

319 One hundred and fifty-two out of 157 zircon grains analysed in sample LCG04 were concordant.  
320 Ages exhibit a wide range from ca.  $233 \pm 3$  Ma to 3.0 Ga; but most fall between 230 Ma to 1050 Ma  
321 (89%). A KDE plot of the data shows a main peak at  $\sim 800$  Ma (49%), and three minor peaks at  $\sim 248$   
322 Ma (5%),  $\sim 510$  Ma (7%) and  $\sim 950$  Ma (14%) ([Fig. 9d](#)).

323 *Late Triassic Maantang, Xiaotangzi and Xujiahe Formations*

324 Two samples (grey sandstone), LCG05 (102°51'34.05"E, 29°40'51.18"N) and LCG06  
325 (102°51'34.05"E, 29°40'51.18"N), were collected from the Maantang Formation and the upper part of  
326 Xujiahe Formation in the Longcanggou section (Fig. 6). For sample LCG05 149 out of 154 single  
327 zircon ages of are concordant. Most ages cluster at ~1800 Ma, with minor peaks at ~250 Ma, ~800 Ma  
328 and ~2500 Ma (Fig. 9e). The age distributions are significantly different from the lower ones (Figs  
329 9a-d). Late Triassic sample LCG06 yielded 99 concordant ages out of 110 analyses. The KDE plot  
330 shows five peaks at ~246 Ma, ~440 Ma, ~758 Ma, ~1870 Ma and ~2480 Ma, respectively (Fig. 9f).

331 Three samples (grey sandstone), CZ05 (103°24'6"E, 29°37'23"N), CZ01 (103°24'22"E,  
332 29°37'20"N), and CZ03 (103°24'43.2"E, 29°37'27"N), were collected from the upper part of the  
333 Xiaotangzi and Xujiahe Formations in the Chuanzhu section (Fig. 6). The KDE plots of these samples  
334 are similar, showing peaks at ~276 Ma, ~429 Ma, ~1030 Ma, ~1860 Ma and ~2470 Ma (Figs 9g-i).

335

## 336 **DISCUSSION**

### 337 **Detrital sources**

#### 338 *Zircon spectra of potential sources*

339 As suggested by previous detrital zircon studies of the Sichuan Basin (Deng *et al.*, 2008;  
340 Weislogel *et al.*, 2010; Chen, 2011; Luo *et al.*, 2014; Zhang *et al.*, 2015a; Shao *et al.*, 2016; Zhu *et al.*,  
341 2017), potential source terrains for the Triassic strata include the eastern Songpan-Ganze terrane,  
342 northern and southern Kangdian, Longmen Shan thrust belt, Qinling orogen, southeastern Yangtze  
343 Block. To facilitate comparison, we compiled zircon U-Pb ages of the pre-late Triassic crystalline and  
344 clastic rocks exposed in these potential source areas (Fig. 10). The detrital zircon U-Pb age spectrum of  
345 the eastern Songpan-Ganze terrane shows three major peaks at ~290 Ma, ~430 Ma, ~1870 Ma, and  
346 two minor peaks at ~770 Ma, ~950 Ma, ~2480 Ma (Fig. 10f). The northern and the southern Kangdian  
347 basement is characterised by different zircon U-Pb age spectra, with the northern part including two  
348 major peaks at ~800 Ma and ~930 Ma and a minor peak at ~260 Ma (Fig. 10g), and the southern part  
349 composed of multiple peaks at ~810 Ma, ~1840 Ma, ~2310 Ma and ~2430 Ma (Fig. 10h). The  
350 Longmen Shan thrust belt produces three major peaks at ~520 Ma, ~750 Ma and, ~945 Ma (Fig. 10i).  
351 The Qinling orogen is characterised by three major peaks at ~440 Ma, ~815 Ma and ~1995 Ma, and  
352 three minor peaks at ~260 Ma, ~1830 Ma and ~2465 Ma (Fig. 10j). The southeastern Yangtze Block  
353 yields a dominant peak at ~815 Ma (Fig. 10k).

354 It is worth noting that ratios between components of the age spectra of potential source areas may  
355 not be representative, even though hundreds of single ages have been compiled. This is because the  
356 spectra are based on only a small number of studies of Neoproterozoic sediments, covering a small part  
357 of the source area (Figs 10g, i and j). For example, the age data of north Kangdian basement are mostly  
358 (336 out of 407 U-Pb ages) derived from the Neoproterozoic Yanbian Group (Zhou *et al.*, 2006a and  
359 Sun *et al.*, 2009), and 37 of the 407 dates are ~800 Ma crystallization ages of Neoproterozoic igneous  
360 rocks, (Fig. 10g). The remaining 34 dates come from an Upper Permian sandstone sample of ~260 Ma,  
361 likely derived from Emeishan igneous province (He *et al.*, 2007). Our data interpretation ignores the

362 proportions of age peaks as these will be affected by zircon fertility and variations in exposure area of  
363 the different rock types across the study area.

#### 364 *Detrital sources of the Early and Middle Triassic strata*

365 Detrital zircon age of four Early and Middle Triassic samples (LCG01, LMD02, LCG03, LCG04)  
366 defines a prominent peak at ~810 Ma. It is worth noting that two of four samples (LCG01, LCG04)  
367 exhibit three minor peaks at ~255 Ma, ~535 Ma and ~970 Ma, which are absent from samples LCG 02  
368 and LMD02 (Fig. 9).

369 The ~810 Ma age peak is present in three potential source areas; the northern Kangdian basement,  
370 the southeastern Yangtze Block and the Longmen Shan. The most likely source is the northern  
371 Kangdian basement. The age spectra of crystalline rocks of the northern Kangdian basement is  
372 dominated by the peak at ~800 Ma, similar to that of Early and Middle Triassic sediments. However,  
373 the bulk age spectra of the northern Kangdian basement also includes a major peak at ~930 Ma, which  
374 forms a minor component in the Early and Middle Triassic sediments. This suggests the  
375 Neoproterozoic meta-sediments of the northern Kangdian were not a major source, probably because  
376 exposure of meta-sediments is relatively limited.

377 The southeastern Yangtze Block cannot be ruled out as a possible source for Early and Middle  
378 Triassic sediments; but the possibility is very low. If the southeastern Yangtze Block were a source, it  
379 would require a long drainage system to deliver the sediments into the southwestern Sichuan Basin via  
380 the northern Kangdian, because the southeastern Yangtze Block and the southwestern Sichuan Basin  
381 were separated by a N-S striking depocenter, running across the central part of the basin (Figs. 4b, c),  
382 where coeval deposits are composed of carbonate, shale and mudstone (Hu, *et al.*, 2010; Tan, *et al.*,  
383 2014; Sun, *et al.*, 2015).

384 The ~810 Ma age mode might also be sourced from the Longmen Shan, even though it does not  
385 form a major age peak therein (Fig. 10i). This interpretation is also supported by the presence of a  
386 minor age peak at ~535 Ma in both the Paleozoic sedimentary rocks of the Longmen Shan and the  
387 Early and Middle Triassic strata in the study area (Figs 10a, i). Such an interpretation in terms of the  
388 source area is also consistent with the eastward paleocurrent directions of these Early and Middle  
389 Triassic sediments (Fig. 5).

390 Further, our Early and Middle Triassic samples also shows a minor peak at ~255 Ma, which  
391 overlaps with the age of the Emeishan basalt (~260 Ma) (He *et al.*, 2007), which is widespread in the  
392 northern Kangdian basement region (Fig. 1). This result supports our interpretation that the Kangdian  
393 basement was a major source for the southwestern Sichuan Basin. The ~255 Ma peak is minor,  
394 probably because of the relatively lower concentration and relatively small grain-size of zircons in  
395 mafic rocks.

396 Last but not least, the above interpretation is also supported by the relatively higher content of  
397 volcanic detritus and the relatively more complex lithic composition in Early Triassic formations  
398 (average 32% of total lithic grains) (Fig. 7). The most likely source of the volcanic clasts is the  
399 Emeishan large igneous province, located south of the Sichuan Basin. The complex lithic  
400 composition may result from the multiple rock types in that region, where metamorphic (slate, phyllite),  
401 volcanic (basalt, rhyolite, andesite, granite) and sedimentary (limestone, dolomite, shale, mudstone,  
402 siltite, sandstone, conglomerate) rocks were preserved (BGMRSF, 1991).

403

405 In contrast to the Early-Middle Triassic samples, detrital zircons from the Late Triassic samples  
406 (LCG05, LCG06, CZ05, CZ01, CZ03), which exhibit southeastward paleocurrent directions (Fig. 5),  
407 give multiple age peaks at ~270 Ma, ~435 Ma, ~775Ma and ~1010 Ma, ~1840Ma and 2480 Ma (Fig.  
408 10b). Detrital zircon data of the coeval sediments in the southwestern, western and northern Sichuan  
409 Basin, as reported in previous studies, yield similar age spectra (Figs 10c, d, e), indicating that they  
410 may share the same or similar sources, that include the Qinling orogen, Longmen Shan thrust belt, and  
411 eastern Songpan-Ganze terrane (Chen, 2011; Luo *et al.*, 2014; Zhang *et al.*, 2015a; Shao *et al.*, 2016).

412 Similar age spectra are seen in the Triassic turbidites of the eastern Songpan-Ganze terrane  
413 (Weislogel *et al.*, 2006, 2010; Enkelmann *et al.*, 2007; Ding *et al.*, 2013; Wang *et al.*, 2013a; Zhang *et al.*,  
414 2014, 2015b), that may have shared similar sources as the Sichuan Basin. Alternatively, the eastern  
415 Songpan-Ganze terrane may have experienced a phase of shortening in response to the Late Triassic  
416 intracontinental orogeny along the Longmen Shan thrust belt (Li *et al.*, 2003a; Yan *et al.*, 2011; Zheng  
417 *et al.*, 2016). From this perspective, it is speculated that the eastern Songpan-Ganze terrane might also  
418 be a source region for the Late Triassic detritus of the Sichuan Basin.

419 Therefore, detritus of the southwestern Sichuan Basin probably changed significantly between  
420 Early and Late Triassic time switching from the Northern Kangdian basement to the Qinling orogeny -  
421 Longmen Shan thrust belt - eastern Songpan-Ganze terrane. Such a change is also supported by the  
422 composition change of sandstone from lithic- to quartz-rich (Fig. 7). This change in Triassic sediment  
423 routing system has significant palaeogeographic and tectonic implications as discussed below.

424

## 425 **Tectonic and palaeogeographic implications**

426 Despite significant change in detrital zircon age spectra, palaeocurrent orientations of the Lower,  
427 Middle and Upper Triassic strata barely changed and are mostly eastward. To account for this the  
428 Kangdian basement, which is now south of the study area, would need to have been located to the west  
429 (Fig. 11a). This requirement, that the basement experienced considerable eastward displacement  
430 relative to the Sichuan Basin, is consistent with the Late Mesozoic and Cenozoic deformation history  
431 of the region: Migration of Mesozoic depocenters in the Sichuan Basin, Meng *et al.* (2005) suggested  
432 that the basin experienced considerable clockwise rotation during Mesozoic time, and Late Cenozoic  
433 left-lateral strike-slip along the Xianshuihe fault displaced the Kangdian basement eastward from the  
434 Longmen Shan by ~80 km (Wang *et al.*, 2009; Tian *et al.*, 2014).

435 A conclusion that Late Triassic sediments in the Sichuan Basin were mainly sourced from the  
436 Qinling orogeny and the Longmen Shan thrust belt is consistent with previous studies (Fig. 11b) (Deng  
437 *et al.*, 2008; Chen, 2011; Luo *et al.*, 2014; Zhang *et al.*, 2015; Shao *et al.*, 2016; Zhu *et al.*, 2017). The  
438 sediment routing system is mostly eastward and southeastward, as indicated by the paleocurrent data  
439 (Fig. 5). The similarity in detrital zircon age distributions between the Late Triassic sediments and the  
440 eastern Songpan-Ganze terrane indicates that the eastern Songpan-Ganze terrane might also have been  
441 significantly shortened and unroofed, providing detritus for the western and southern Sichuan Basin.  
442 The Late Triassic shortening of the Songpan-Ganze turbidites might relate to several possible processes,  
443 including (1) westward subduction of the Ganze-Litang Ocean during the Late Triassic (Hou *et al.*,  
444 2004), (2) collision between Yidun arc and the Songpan-Ganze terrane at the end of the Triassic (Hou  
445 *et al.*, 2004; Wang *et al.*, 2013a), (3) intra-continental transpressional shortening between the eastern

446 Songpan-Ganze terrane and the Sichuan Basin, forming the Longmen Shan thrust belt(e.g. Li *et al.*,  
447 2003a; Harrowfield & Wilson, 2005; Wang & Meng, 2008), and (4) slab retreat or rollback of  
448 Paleo-Tethys lithosphere (e.g. de Sigoyer *et al.*, 2014; Pullen *et al.*, 2008; Zhang *et al.*, 2015c).

449 Late Triassic uplift and unroofing of the Longmen Shan thrust belt is required to provide detritus  
450 for the Late Triassic deposits, as discussed above. This speculation is consistent with other lines of  
451 evidence. First, the presence of klippen of Paleozoic and Precambrian rocks over Triassic sediments in  
452 the eastern front of the Longmen Shan thrust belt indicate that these structures were formed during the  
453 Late Triassic or later. Second, the oldest U–Th–Pb monazite and Sm–Nd garnet ages (204–190 Ma),  
454 derived from metamorphosed rocks in the Danba Antiform, immediately south of the Longmen Shan  
455 thrust belt, were interpreted as dating the timing of Barrovian metamorphism associated with  
456 deformation (Huang *et al.*, 2003; Weller *et al.*, 2013). Third, muscovite  $^{40}\text{Ar}/^{39}\text{Ar}$  dating of Early  
457 Paleozoic schist and Neoproterozoic Pengguan complex from the northern and middle Longmen Shan  
458 yielded ages between 237–208 Ma and 235–226 Ma, respectively, which were interpreted as minimum  
459 age constraints for Mesozoic crustal shortening (Yan *et al.*, 2011; Zheng *et al.*, 2016).

460 As indicated by our palaeocurrent and detrital zircon results, the northern Kangdian basement was  
461 uplifted and unroofed to provide the detritus for the Early and Middle Triassic sediments in the  
462 southwestern Sichuan Basin (Fig. 11a). However, in Late Triassic time, the basement subsided  
463 significantly in Late Triassic time (Fig. 11b), as indicated by the presence of Late Triassic sediments  
464 (~1 km, Guo *et al.*, 1996) over the basement rocks (Fig. 2). Subsidence of the basement might result  
465 from eastward shortening and loading of the eastern Songpan-Ganze terrane over the western margin of  
466 the Yangtze Block in response to the Late Triassic collision between the Yangtze Block, Yidun arc and  
467 Qiangtang terrane along the Ganze-Litang and Jinshajiang sutures (Fig. 11b). This interpretation is also  
468 supported by the eastward paleocurrent and the development of a ~1.5-km-thick Late Triassic  
469 depocenter in areas south of the sampling sites (i.e. the location of the northern Kangdian basement)  
470 (Fig. 4a). Such a tectonic reconstruction differs from previous models, suggesting continuous Late  
471 Permian to Jurassic subsidence related to rifting (Luo, 1983; Guo *et al.*, 1996), or early Mesozoic  
472 transensional subsidence by strike-slip faulting (Chen *et al.*, 1987; He *et al.*, 2003; Chen *et al.*, 2011).

473

## 474 CONCLUSIONS

475 Triassic sediments in the southwestern Sichuan Basin record different detrital zircon  
476 geochronology signals. Detrital zircon age spectra of Early and Middle Triassic samples are  
477 characterized by a dominant age mode at ~810 Ma, with three minor peaks at ~255Ma, ~535Ma and  
478 ~970Ma. In contrast to the Early -Middle Triassic samples, detrital zircon spectra of Upper Triassic  
479 samples are characterized by multiple age peaks at ~270 Ma, ~435 Ma, ~775Ma and ~1010 Ma,  
480 ~1840Ma and ~2480 Ma.

481 Our data reveal a major change of provenance during the Late Triassic in response to multiple  
482 tectonic events. Sediments in the southwestern Sichuan Basin was supplied by highlands of the  
483 Yangtze Block (the northern Kangdian basement) during the Early-Middle Triassic passive continental  
484 margin stage. During the Late Triassic, the Sichuan Basin was inverted into a foreland basin and the  
485 Longmen Shan thrust belt and possibly the eastern Songpan-Ganze terrane was uplifted in response to  
486 the closure of the Paleo-Tethys Ocean and intra-continental shortening. Together with the Qinling  
487 orogen, they became the main source areas for the southwestern and western Sichuan Basin. The Late

488 Triassic sediments in the southwestern Sichuan Basin have thus recorded collision and subsequent  
489 convergence between the Qiangtang, Yangtze and North China blocks. This study highlights the  
490 importance of tectonic events in reorganizing drainage and sediment supply in a foreland basin system.

491 Further, during the Late Triassic the northern Kangdian basement region was inverted and then  
492 switched from an area undergoing uplift and erosion into a region of subsidence, probably due to the  
493 eastward shortening and loading of the Songpan-Ganze terrane over the western margin of the Yangtze  
494 Block in response to the Late Triassic collision between Yangtze Block, Yidun arc and Qiangtang  
495 terrane along the Ganze-Litang and Jinshajiang sutures.

496  
497

## 498 **ACKNOWLEDGEMENTS**

499 We thank Yan Liang, Yun Kun, Chen Bin, Wang Weiming, Lu Yanqi and Zhou Qiwei for their  
500 help in the field. This work benefited from discussions with Profs. Hu Xiumian, Dr. Dong Shunli and  
501 Dr. Chen Yang. Funding for this research was provided by National Natural Science Foundation of  
502 China (Grant No. 41502116, 41772211, 41372114 and 41340005), Chinese 1000 Young Talents  
503 Program and the National Key Laboratory of Oil and Gas Reservoir Geology and Exploitation (Grant  
504 No. PLC201604). Constructive reviews by Drs. Amy Weislogel, Alex Pullen, Guanwei Li, Paul  
505 Eizenhöfer and an anonymous reviewer, and the editor Dr. Nadine McQuarrie clarified many points in  
506 this article.

## 507 **REFERENCES**

- 508 BGMRSP (Bureau of Geology and Mineral Resources, Sichuan Province), (1991). Regional Geology  
509 of Sichuan Province. Geological Publishing House, Beijing, in Chinese.
- 510 BGMRSP (Bureau of Geology and Mineral Resources, Sichuan Province), (1997). Multiple  
511 stratigraphic division research in China: lithostratigraphy in Sichuan Province. China University  
512 of Geosciences Press, Wuhan, 1-417 pp, in Chinese.
- 513 BGSP (Bureau of Geology, Sichuan Province), (1974). Bureau of Geology and Mineral Resources of  
514 Sichuan Province. Regional Geological Report of Yingjing Sheet (1:200000). Geological  
515 Publishing House, Beijing, 1-143 pp, in Chinese.
- 516 BURCHFIEL, B.C., CHEN, Z., LIU, Y. & ROYDEN, L.H. (1995) Tectonics of the Longmen Shan and  
517 adjacent regions, central China. *International Geology Review*, **37**, 661-735.
- 518 BURGESS, S.D., BOWRING, S.A. & SHEN, S. (2014) High-precision timeline for Earth's most severe  
519 extinction. *Proceedings of the National Academy of Sciences of the United States of America*, **111**,  
520 3316-3321.
- 521 CHANG, E.Z. (2000) Geology and tectonics of the Songpan-Ganzi fold belt, southwestern China.  
522 *International Geology Review*, **42**, 813-831.
- 523 CHEN, H., ZHANG, C., HUANG, F. & HOU, M. (2011) Filling process and evolutionary model of  
524 sedimentary sequence of Middle-Upper Yangtze craton in Hercynian-Indosinian  
525 (Devonian-Middle Triassic). *Acta Petrologica Sinica*, **27**, 2281-2298, in Chinese with English  
526 abstract.
- 527 CHEN, Q., SUN, M., LONG, X., ZHAO, G. & YUAN, C. (2016) U - Pb ages and Hf isotopic record of  
528 zircons from the late Neoproterozoic and Silurian - Devonian sedimentary rocks of the western  
529 Yangtze Block: Implications for its tectonic evolution and continental affinity. *Gondwana  
530 Research*. **31**, 184-199..
- 531 CHEN, Y. (2011) The Formation of Wesatern Sichuan Foreland Basin and Its Significance in Oil-gas  
532 Exploration During Late Triassic, Chengdu University of Technology, Chengdu, 1-170 pp, in  
533 Chinese with English abstract.
- 534 CHEN, Z. & CHEN, S. (1987) *On the tectonic evolution of the West Margin of the Yangzi Block*.  
535 Chongqing Publishing House, Chongqing.

- 536 DAI, S., REN, D., CHOU, C., FINKELMAN, R.B., SEREDIN, V.V. & ZHOU, Y. (2012) Geochemistry of  
537 trace elements in Chinese coals: A review of abundances, genetic types, impacts on human health,  
538 and industrial utilization. *International Journal of Coal Geology*, **94**, 3-21.
- 539 DE SIGOYER, J., VANDERHAEGHE, O., DUCHÈNE, S. & BILLEROT, A. (2014) Generation and  
540 emplacement of Triassic granitoids within the Songpan Ganze accretionary-orogenic wedge in a  
541 context of slab retreat accommodated by tear faulting, Eastern Tibetan plateau, China. *Journal of*  
542 *Asian Earth Sciences*, **88**, 192-216.
- 543 DECELLES, P.G., LANGFORD, R.P. & SCHWARTZ R. K. (1983) Two new methods of paleocurrent  
544 determination from trough cross-stratification. *Journal of Sedimentary Research*, **53**: 629-642
- 545 DENG, F., JIA, D., LUO, L., LI, H., LI, Y. & WU, L. (2008) The contrast between provenances of  
546 Songpan-Ganze and Western Sichuan foreland basin in the Late Triassic: clues to the tectonics  
547 and palaeogeography. *Geological Review*, **54**, 561-573, in Chinese with English abstract.
- 548 DING, L., YANG, D., CAI, F.L., PULLEN, A., KAPP, P., GEHRELS, G.E., ZHANG, L.Y., ZHANG, Q.H., LAI,  
549 Q.Z., YUE, Y.H. & SHI, R.D. (2013) Provenance analysis of the Mesozoic  
550 Hoh-Xil-Songpan-Ganze turbidites in northern Tibet: Implications for the tectonic evolution of the  
551 eastern Paleo-Tethys Ocean. *Tectonics*, **32**, 34-48.
- 552 DUAN, L., MENG, Q., ZHANG, C. & LIU, X. (2011) Tracing the position of the South China block in  
553 Gondwana: U - Pb ages and Hf isotopes of Devonian detrital zircons. *Gondwana Research*, **19**,  
554 141-149.
- 555 ENKELMANN, E., RATSCHBACHER, L., JONCKHEERE, R., NESTLER, R., FLEISCHER, M., GLOAGUEN, R.,  
556 HACKER, B.R., ZHANG, Y.Q. & MA, Y.S. (2006) Cenozoic exhumation and deformation of  
557 northeastern Tibet and the Qinling: Is Tibetan lower crustal flow diverging around the Sichuan  
558 Basin? *Geological Society of America Bulletin*, **118**, 651-671.
- 559 ENKELMANN, E., WEISLOGEL, A., RATSCHBACHER, L., EIDE, E., RENNO, A. & WOODEN, J. (2007) How  
560 was the Triassic Songpan-Ganze basin filled? A provenance study. *Tectonics*, **26**, n/a-n/a.
- 561 FENG, Z., BAO, Z. & LI, S. (1997) Potential of oil and gas of the Middle and Lower Triassic of south  
562 China from the viewpoint of lithofacies paleogeography. *Journal of the University of Petroleum* ,  
563 *China*, **21**, 1-6, in Chinese with English abstract.
- 564 FENG, Z., JIN, Z., HE, Y., BAO, Z. & XIN, W. (1994) *Lithofacies paleogeography of Permian of*  
565 *Yunnan-Guizhou-Guangxi Region*. Geological Publishing House, Beijing, 1-146 pp, in Chinese  
566 with English abstract.
- 567 FU, B., KITA, N.T., WILDE, S.A., LIU, X., CLIFF, J. & GREIG, A. (2013) Origin of the  
568 Tongbai-Dabie-Sulu Neoproterozoic low- $\delta$  18O igneous province, east-central China.  
569 *Contributions to Mineralogy and Petrology*, **165**, 641-662.
- 570 GARZANTI, E. (2016) From static to dynamic provenance analysis—Sedimentary petrology upgraded.  
571 *Sedimentary Geology*, **336**, 3-13.
- 572 GENG, Y., YANG, C., WANG, X. & LIUDONG, R. (2007) Age of Crystalline basement in Western Margin  
573 of Yangtze Terrane. *Geological Journal of China Universities*, **13**, 429-441, in Chinese with  
574 English abstract.
- 575 GRADSTEIN, F.M., OGG, J.G., SCHMITZ, M. & OGG, G. (2012) The Geologic Time Scale 2012  
576 2-Volume Set.
- 577 GRIFFIN, W.L., POWELL, W.J., PEARSON, N.J., O'REILLY, S.Y. & A, E.M. (2008) GLITTER: data  
578 reduction software for laser ablation ICP-MS. In: *Laser Ablation-ICP-MS in the earth sciences*  
579 (Ed. by P. S. ED.), **40**, 204-207. Mineralogical association of Canada short course series.
- 580 GUO, J., YOU, Z., YANG, J., SHEN, W., XU, S. & WANG, R. (1998) Studying on the U-Pb dating of  
581 zircon in Tianwan and Pianlugang bodies from Shimian area, west Sichuan. *Journal of*  
582 *Mineralogy and Petrology*, **18**, 92-95, in Chinese with English abstract.
- 583 GUO, Z., DENG, K., HAN, Y. & LIU, Y. (1996) *The Formation and Development of Sichuan Basin*.  
584 Geological Publishing House, Beijing, 1-200 pp, in Chinese with English abstract.
- 585 HARROWFIELD, M.J. & WILSON, C.J.L. (2005) Indosinian deformation of the Songpan Garzê Fold Belt,  
586 northeast Tibetan Plateau. *Journal of Structural Geology*, **27**, 101-117.
- 587 HE, B., XU, Y., HUANG, X., LUO, Z., SHI, Y., YANG, Q. & YU, S. (2007) Age and duration of the  
588 Emeishan flood volcanism, SW China: Geochemistry and SHRIMP zircon U-Pb dating of silicic  
589 ignimbrites, post-volcanic Xuanwei Formation and clay tuff at the Chaotian section. *Earth and*  
590 *Planetary Science Letters*, **255**, 306-323.
- 591 HE, B., XU, Y., XIAO, L. & WANG, Y. (2003) Does the Panzhihua-Xichang Rift Exist? *Geological*  
592 *Review*, **49**, 572-582, in Chinese with English abstract.
- 593 HOU, Z., YANG, Y., QU, X., HUANG, D., LU, Q., WANG, H., YU, J. & TANG, S. (2004) Tectonic  
594 evolution and mineralization systems of the Yidun Arc orogen in Sanjiang region, China. *Acta*  
595 *Geologica Sinica*, **78**, 109-120, in Chinese with English abstract.

- 596 HU, M., WEI, G., LI, S., YANG, W., ZHU, L. & YANG, Y. (2010) Characteristics of Sequence-based  
597 Lithofacies and Paleogeography, and Reservoir Prediction of the Jialingjiang Formation in  
598 Sichuan Basin. *Acta Sedimentologica Sinica*, **28**, 1145-1152, in Chinese with English abstract.
- 599 HUANG, M., BUICK, I.S. & HOU, L.W. (2003) Tectonometamorphic Evolution of the Eastern Tibet  
600 Plateau: Evidence from the Central Songpan - Garzê Orogenic Belt, Western China. *Journal of*  
601 *Petrology*, **44**, 255-278.
- 602 HUANG, X., XU, Y., LAN, J., YANG, Q. & LUO, Z. (2009) Neoproterozoic adakitic rocks from  
603 Mopanshan in the western Yangtze Craton: Partial melts of a thickened lower crust. *Lithos*, **112**,  
604 367-381.
- 605 JACKSON, S.E., PEARSON, N.J., GRIFFIN, W.L. & BELOUSOVA, E.A. (2004) The application of laser  
606 ablation-inductively coupled plasma-mass spectrometry to in situ U - Pb zircon geochronology.  
607 *Chemical Geology*, **211**, 47-69.
- 608 JIA, D., WEI, G., CHEN, Z., LI, B., ZENG, Q. & YANG, G. (2006) Longmen Shan fold-thrust belt and its  
609 relation to the western Sichuan Basin in central China: New insights from hydrocarbon  
610 exploration. *Bulletin*, **90**, 1425-1447.
- 611 JIANG, Z., TIAN, J., CHEN, G., LI, X. & ZHANG, M. (2007) Sedimentary characteristics of the Upper  
612 Triassic in western Sichuan foreland basin. *Journal of Palaeogeography*, **9**, 143-154, in Chinese  
613 with English abstract.
- 614 JOCHUM, K.P., WEIS, U., STOLL, B., KUZMIN, D., YANG, Q., RACZEK, I., JACOB, D.E., STRACKE, A.,  
615 BIRBAUM, K., FRICK, D.A., GÜNTHER, D. & ENZWEILER, J. (2011) Determination of Reference  
616 Values for NIST SRM 610-617 Glasses Following ISO Guidelines. *Geostandards and*  
617 *Geoanalytical Research*, **35**, 397-429.
- 618 LEHRMANN, D.J., STEPCHINSKI, L., ALTINER, D., ORCHARD, M.J., MONTGOMERY, P., ENOS, P.,  
619 ELLWOOD, B.B., BOWRING, S.A., RAMEZANI, J. & WANG, H. (2015) An integrated biostratigraphy  
620 (conodonts and foraminifers) and chronostratigraphy (paleomagnetic reversals, magnetic  
621 susceptibility, elemental chemistry, carbon isotopes and geochronology) for the Permian - Upper  
622 Triassic strata of Guandao section, Nanpanjiang Basin, south China. *Journal of Asian Earth*  
623 *Sciences*, **108**, 117-135.
- 624 LI, C. (1963) A preliminary study of the tectonic development of the "Kang-Dian Axis". *Acta*  
625 *Geologica Sinica*, **43**, 214-229, in Chinese with English abstract.
- 626 LI, X., LI, Z., ZHOU, H., LIU, Y. & KINNY, P.D. (2002) U - Pb zircon geochronology, geochemistry and  
627 Nd isotopic study of Neoproterozoic bimodal volcanic rocks in the Kangdian Rift of South China:  
628 implications for the initial rifting of Rodinia. *Precambrian Research*, **113**, 135-154.
- 629 LI, X., ZHOU, H., LI, Z., LIU, Y. & P., K. (2001) Zircon U-Pb age and petrochemical characteristics of  
630 the Neoproterozoic bimodal volcanics from western Yangtze block. *Geochimica*, **30**, 315-322, in  
631 Chinese with English abstract.
- 632 LI, Y., ALLEN, P.A., DENSMORE, A.L. & QIANG, X. (2003a) Evolution of the Longmen Shan foreland  
633 basin (western Sichuan, China) during the Late Triassic Indosinian orogeny. *Basin Research*, **15**,  
634 117-138.
- 635 LI, Y., HE, D., LI, D., WEN, Z., MEI, Q., LI, C. & SUN, Y. (2016) Detrital zircon U-Pb geochronology  
636 and provenance of Lower Cretaceous sediments: Constraints for the northwestern Sichuan  
637 pro-foreland basin. *Palaeogeography, Palaeoclimatology, Palaeoecology*, **453**, 52-72.
- 638 LI, Y., YAN, Z., LIU, S., LI, H., CAO, J., SU, D., DONG, S., SUN, W., YANG, R. & YAN, L. (2014)  
639 Migration of the carbonate ramp and sponge buildup driven by the orogenic wedge advance in the  
640 early stage (Carnian) of the Longmen Shan foreland basin, China. *Tectonophysics*, **619-620**,  
641 179-193.
- 642 LI, Z.X., LI, X.H., KINNY, P.D., WANG, J., ZHANG, S. & ZHOU, H. (2003b) Geochronology of  
643 Neoproterozoic syn-rift magmatism in the Yangtze Craton, South China and correlations with  
644 other continents: evidence for a mantle superplume that broke up Rodinia. *Precambrian Research*,  
645 **122**, 85-109.
- 646 LIN, G. (2010) Zircon U-Pb age and petrochemical characteristics of Shimian granite in western  
647 Sichuan: petrogenesis and tectonic significance. *Earth Science-Journal of China University of*  
648 *Geoscience*, **35**, 611-620, in Chinese with English abstract.
- 649 LIN, G., LI, X. & LI, W. (2006) SHRIMP U-Pb zircon age, geochemistry and Nd-Hf isotope of  
650 Neoproterozoic mafic dyke swarms in western Sichuan: Petrogenesis and tectonic significance.  
651 *SCIENCE CHINA: Earth Sciences*, **36**, 630-645, in Chinese with English abstract.
- 652 LIN, W., WANG, H. & SONG, H. (1982) Upper Permian to Lower-middle Trisassic Strata and  
653 Sedimentary Environments in Longmendong, Emei, Sichuan. *Journal of Mineralogy and*  
654 *Petrology*, 53-58.



- 655 LIU, S., STEEL, R. & ZHANG, G. (2005) Mesozoic sedimentary basin development and tectonic  
656 implication, northern Yangtze Block, eastern China: record of continent–continent collision.  
657 *Journal of Asian Earth Sciences*, **25**, 9-27.
- 658 LIU, S., MA, P., YAO, X., LIN, C. & QIAN, T. (2015) Oblique closure of the northeastern Paleo-Tethys  
659 in central China. *Tectonics*, **3**, 413-434.
- 660 LIU-ZENG, J., TAPPONNIER, P., GAUDEMER, Y. & DING, L. (2008) Quantifying landscape differences  
661 across the Tibetan plateau: Implications for topographic relief evolution. *Journal of Geophysical*  
662 *Research: Earth Surface*, **113**.
- 663 LIU, Z. & TONG, J. (2001) The Middle Triassic Stratigraphy and Sedimentary Paleogeography of South  
664 China. *Acta Sedimentologica Sinica*, **19**, 327-332, in Chinese with English abstract.
- 665 LONG, S., WU, S., LI, H., BAI, Z., MA, J. & ZHANG, H. (2011) Hybrid sedimentation in Late  
666 Permian-Early Triassic in western Sichuan basin, China. *J. Earth Sci.*, **22**, 340-350.
- 667 LUO, L., QI, J., ZHANG, M., WANG, K. & HAN, Y. (2014) Detrital zircon U–Pb ages of Late Triassic –  
668 Late Jurassic deposits in the western and northern Sichuan Basin margin: constraints on the  
669 foreland basin provenance and tectonic implications. *Int J Earth Sci (Geol Rundsch)*, **103**,  
670 1553-1568.
- 671 LUO, Y. (1983) The evolution of paleoplates in the Kang-Dian tectonic zone. *Earth Science-Journal of*  
672 *Wuhan College of Geology*, **22**, 93-102, in Chinese with English abstract.
- 673 MENG, E., LIU, F., DU, L., LIU, P. & LIU, J. (2015) Petrogenesis and tectonic significance of the  
674 Baoping granitic and mafic intrusions, southwestern China: Evidence from zircon U–Pb dating  
675 and Lu – Hf isotopes, and whole-rock geochemistry. *Gondwana Research*, **28**, 800-815.
- 676 MENG, Q. & ZHANG, G. (2000) Geologic framework and tectonic evolution of the Qinling orogen,  
677 central China. *Tectonophysics*, **323**, 183-196.
- 678 MENG, Q., WANG, E. & HU, J. (2005) Mesozoic sedimentary evolution of the northwest Sichuan basin:  
679 Implication for continued clockwise rotation of the South China block. *Geol Soc America Bull*,  
680 **117**, 396.
- 681 OVTCHAROVA, M., BUCHER, H., SCHALTEGGER, U., GALFETTI, T., BRAYARD, A. & GUEX, J. (2006)  
682 New Early to Middle Triassic U–Pb ages from South China: Calibration with ammonoid  
683 biochronozones and implications for the timing of the Triassic biotic recovery. *Earth and*  
684 *Planetary Science Letters*, **243**, 463-475.
- 685 PULLEN, A., KAPP, P., GEHRELS, G.E., VERVOORT, J.D. & DING, L. (2008) Triassic continental  
686 subduction in central Tibet and Mediterranean-style closure of the Paleo-Tethys Ocean. *Geol*, **36**,  
687 351.
- 688 REID, A.J., WILSON, C.J.L. & LIU, S. (2005) Structural evidence for the Permo-Triassic tectonic  
689 evolution of the Yidun Arc, eastern Tibetan Plateau. *Journal of Structural Geology*, **27**, 119-137.
- 690 RITTNER, M., VERMEESCH, P., CARTER, A., BIRD, A., STEVENS, T., GARZANTI, E., ANDÒ,  
691 S., VEZZOLI, G., DUTT, R., XU, Z. & LU, H. (2016) The Provenance of Taklamakan Desert  
692 Sand. *Earth and Planetary Science Letters*, 437, 127-137.
- 693 ROGER, F. & CALASSOU, S. (1997) Géochronologie U-Pb sur zircons et géochimie (Pb, Sr et Nd) du  
694 socle de la chaîne de Songpan-Garze (Chine). *Comptes Rendus de l'Académie des Sciences-Series*  
695 *IIA-Earth and Planetary Science*, **324**, 819-826.
- 696 ROGER, F., JOLIVET, M. & MALAVIEILLE, J. (2010) The tectonic evolution of the Songpan-Garzê  
697 (North Tibet) and adjacent areas from Proterozoic to Present: A synthesis. *Journal of Asian Earth*  
698 *Sciences*, **39**, 254-269.
- 699 ROGER, F., JOLIVET, M., CATTIN, R. & MALAVIEILLE, J. (2011) Mesozoic-Cenozoic tectonothermal  
700 evolution of the eastern part of the Tibetan Plateau (Songpan-Garze, Longmen Shan area):  
701 insights from thermochronological data and simple thermal modelling. *Geological Society,*  
702 *London, Special Publications*, **353**, 9-25.
- 703 ROGER, F., JOLIVET, M. & MALAVIEILLE, J. (2008) Tectonic evolution of the Triassic fold belts of  
704 Tibet. *Comptes Rendus Geoscience*, **340**, 180-189.
- 705 ROGER, F., MALAVIEILLE, J., LELOUP, P.H., CALASSOU, S. & XU, Z. (2004) Timing of granite  
706 emplacement and cooling in the Songpan–Garzê Fold Belt (eastern Tibetan Plateau) with tectonic  
707 implications. *Journal of Asian Earth Sciences*, **22**, 465-481.
- 708 RUAN, L. (2013) The Metallogenic Regularity of Dashuigou Tellurium Deposit, Shimian, Sichuan  
709 Province and the Origination of Prospecting, China University of Geosciences, Wuhan, in Chinese  
710 with English abstract.
- 711 SHAO, T., CHENG, N. & SONG, M. (2016) Provenance and tectonic-paleogeographic evolution:  
712 Constraints from detrital zircon U – Pb ages of Late Triassic-Early Jurassic deposits in the

- 713 northern Sichuan basin, central China. *Journal of Asian Earth Sciences*, **127**, 12-31.
- 714 SHEN, W., GAO, J., XU, S., LI, H., ZHOU, G., YANG, Z. & YANG, Q. (2003) Geochemical Characteristics  
715 of the Shimian Ophiolite, Sichuan Province and Its Tectonic Significance. *Geological Review*, **49**,  
716 17-27, in Chinese with English abstract.
- 717 SHEN, W., LI, H., XU, S. & WANG, R. (2000) U-Pb Chronological Study of Zircons from the  
718 Huangcaoshan and Xiasuozi Granites in the Western Margin of Yangtze Plate. *Geological Journal*  
719 *of China Universities*, **6**, 412-416, in Chinese with English abstract.
- 720 SHI, Z., PRETO, N., JIANG, H., KRYSSTYN, L., ZHANG, Y., OGG, J.G., JIN, X., YUAN, J., YANG, X. & DU,  
721 Y. (2016) Demise of Late Triassic sponge mounds along the northwestern margin of the Yangtze  
722 Block, South China: Related to the Carnian Pluvial Phase? *Palaeogeography Palaeoclimatology*  
723 *Palaeoecology*.
- 724 SHI, Z., YANG, W., XIE, Z., JIN, H. & XIE, W. (2010) Upper Triassic Clastic Composition in Sichuan  
725 Basin, Southwest China: Implication for Provenance Analysis and the Indosinian Orogeny. *ACTA*  
726 *GEOLOGICA SINICA*, **84**, 387-397, in Chinese with English abstract.
- 727 SLÁMA, J., KOŠLER, J., CONDON, D.J., CROWLEY, J.L., GERDES, A., HANCHAR, J.M., HORSTWOOD,  
728 M.S.A., MORRIS, G.A., NASDALA, L., NORBERG, N., SCHALTEGGER, U., SCHOENE, B., TUBRETT,  
729 M.N. & WHITEHOUSE, M.J. (2008) Plešovice zircon – A new natural reference material for U – Pb  
730 and Hf isotopic microanalysis. *Chemical Geology*, **249**, 1-35.
- 731 SUN, C., HU, M., HU, Z., XUE, D. & WANG, Z. (2015) Sequence-based Lithofacies and Paleogeography  
732 of Lower Triassic Feixianguan Formation in Sichuan Basin. *Marine Origin Petroleum Geology*,  
733 1-9, in Chinese with English abstract.
- 734 SUN, W., ZHOU, M., GAO, J., YANG, Y., ZHAO, X. & ZHAO, J. (2009) Detrital zircon U – Pb  
735 geochronological and Lu – Hf isotopic constraints on the Precambrian magmatic and crustal  
736 evolution of the western Yangtze Block, SW China. *Precambrian Research*, **172**, 99-126.
- 737 TAN, X., LI, L., LIU, H., CAO, J., WU, X., ZHOU, S. & SHI, X. (2014) Mega-shoaling in carbonate  
738 platform of the Middle Triassic Leikoupo Formation, Sichuan Basin, southwest China. *Sci. China*  
739 *Earth Sci.*, **57**, 465-479.
- 740 TAN, X., XIA, Q., CHEN, J., LI, L., LIU, H., LUO, B., XIA, J. & YANG, J. (2013) Basin-scale sand  
741 deposition in the Upper Triassic Xujiahe formation of the Sichuan Basin, Southwest China:  
742 Sedimentary framework and conceptual model. *Journal of Earth Science*, **24**, 89-103.
- 743 TIAN, Y., KOHN, B.P., GLEADOW, A.J.W. & HU, S. (2013) Constructing the Longmen Shan eastern  
744 Tibetan Plateau margin: Insights from low-temperature thermochronology. *Tectonics*, **32**,  
745 576-592.
- 746 TIAN, Y., KOHN, B.P., PHILLIPS, D., HU, S., GLEADOW, A.J.W. & CARTER, A. (2016) Late  
747 Cretaceous-earliest Paleogene deformation in the Longmen Shan fold-and-thrust belt, eastern  
748 Tibetan Plateau margin: Pre-Cenozoic thickened crust? *Tectonics*, **35**, 2293-2312.
- 749 TIAN, Y., KOHN, B.P., ZHU, C., XU, M., HU, S. & GLEADOW, A.J.W. (2012) Post-orogenic evolution of  
750 the Mesozoic Micang Shan Foreland Basin system, central China. *Basin Research*, **24**, 70-90.
- 751 TIAN, Y., KOHN, B.P., GLEADOW, A.J.W. & HU, S. (2014) A thermochronological perspective on the  
752 morphotectonic evolution of the southeastern Tibetan Plateau. *J. Geophys. Res. Solid Earth*, **119**,  
753 676-698.
- 754 VERMEESCH, P. (2012) On the visualisation of detrital age distributions. *Chemical Geology*, **312-313**,  
755 190-194.
- 756 WANG, B., WANG, W., CHEN, W.T., GAO, J., ZHAO, X., YAN, D. & ZHOU, M. (2013a) Constraints of  
757 detrital zircon U – Pb ages and Hf isotopes on the provenance of the Triassic Yidun Group and  
758 tectonic evolution of the Yidun Terrane, Eastern Tibet. *Sedimentary Geology*, **289**, 74-98.
- 759 WANG, E. & MENG, Q. (2008) Mesozoic and Cenozoic tectonic evolution of the Longmen Shan fault  
760 belt. *Science in CHINA (Series D)*, **38**, 1221-1233.
- 761 WANG, E., KIRBY, E., FURLONG, K.P., VAN SOEST, M., XU, G., SHI, X., KAMP, P.J.J. & HODGES, K.V.  
762 (2012a) Two-phase growth of high topography in eastern Tibet during the Cenozoic. *Nature*  
763 *Geosci*, **5**, 640-645.
- 764 WANG, H., YANG, S. & LI, S. (1983) Mesozoic and Cenozoic basin formation in east China and  
765 adjacent regions and development of the continental margin. *Acta Geologica Sinica*, 213-223, in  
766 Chinese with English abstract.
- 767 WANG, L. & PAN, G. (2013) *Geological Map of the Qinghai-Tibet plateau and adjacent areas*.  
768 Geologied Publishing House, Beijing, in Chinese.
- 769 WANG, L., GRIFFIN, W.L., YU, J. & O REILLY, S.Y. (2010) Precambrian crustal evolution of the  
770 Yangtze Block tracked by detrital zircons from Neoproterozoic sedimentary rocks. *Precambrian*  
771 *Research*, **177**, 131-144.

- 772 WANG, L., GRIFFIN, W.L., YU, J. & O'REILLY, S.Y. (2013b) U-Pb and Lu-Hf isotopes in detrital zircon  
773 from Neoproterozoic sedimentary rocks in the northern Yangtze Block: implications for  
774 Precambrian crustal evolution. *Gondwana Research*, **23**, 1261-1272.
- 775 WANG, L., LU, Y., ZHAO, S. & LUO, J. (1994) *Permian Lithofacies, Paleogeography and*  
776 *Mineralization in South China*. Geological Publishing House, Beijing, 1-156pp, in Chinese with  
777 English abstract.
- 778 WANG, L., YU, J., GRIFFIN, W.L. & O'REILLY, S.Y. (2012b) Early crustal evolution in the western  
779 Yangtze Block: evidence from U - Pb and Lu - Hf isotopes on detrital zircons from sedimentary  
780 rocks. *Precambrian Research*, **222**, 368-385.
- 781 WANG, S., FANG, X., ZHENG, D. & WANG, E. (2009) Initiation of slip along the Xianshuihe fault zone,  
782 eastern Tibet, constrained by K/Ar and fission-track ages. *International Geology Review*, **51**,  
783 1121-1131.
- 784 WANG, W., LI, F. & BAO, Z. (2007) U-Pb Constraints on Provenance and Evolution of Middle to Late  
785 Triassic Sediment in Songpan-Garze Basin. *Geological Science and Technology Information*, **26**,  
786 35-44, in Chinese with English abstract.
- 787 WANG, W. & ZHOU, M. (2012) Sedimentary records of the Yangtze Block (South China) and their  
788 correlation with equivalent Neoproterozoic sequences on adjacent continents. *Sedimentary*  
789 *Geology*, **265-266**, 126-142.
- 790 WANG, Y., ZHANG, Y., FAN, W. & PENG, T. (2005) Structural signatures and  $40\text{ Ar}/39\text{ Ar}$   
791 geochronology of the Indosinian Xuefengshan tectonic belt, South China Block. *Journal of*  
792 *Structural Geology*, **27**, 985-998.
- 793 WEI, Y., ZHANG, Z., HE, W., WU, N. & YANG, B. (2014) Evolution of Sedimentary Basins in the Upper  
794 Yangtze during Mesozoic. *Editorial Committee of Earth Science-Journal of China University of*  
795 *Geosciences*, 1065-1078 in Chinese with English abstract.
- 796 WEISLOGEL, A.L. (2008) Tectonostratigraphic and geochronologic constraints on evolution of the  
797 northeast Paleotethys from the Songpan-Ganze complex, central China. *Tectonophysics*, **451**,  
798 331-345.
- 799 WEISLOGEL, A.L., GRAHAM, S.A., CHANG, E.Z., WOODEN, J.L., GEHRELS, G.E. & YANG, H. (2006)  
800 Detrital zircon provenance of the Late Triassic Songpan-Ganzi complex: Sedimentary record of  
801 collision of the North and South China blocks. *Geology*, **34**, 97-100.
- 802 WEISLOGEL, A.L., GRAHAM, S.A., CHANG, E.Z., WOODEN, J.L. & GEHRELS, G.E. (2010) Detrital  
803 zircon provenance from three turbidite depocenters of the Middle-Upper Triassic Songpan-Ganze  
804 complex, central China: Record of collisional tectonics, erosional exhumation, and sediment  
805 production. *Geological Society of America Bulletin*, **122**, 2041-2062.
- 806 WELLER, O.M., STONGE, M.R., WATERS, D.J., RAYNER, N., SEARLE, M.P., CHUNG, S.L., PALIN, R.M.,  
807 LEE, Y. & XU, X. (2013) Quantifying Barrovian metamorphism in the Danba Structural  
808 Culmination of eastern Tibet. *Journal of Metamorphic Geology*, **31**, 909-935.
- 809 WGCMSPIB (Write Group of Continental Mesozoic Stratigraphy and Paleontology in Sichuan Basin  
810 of China) (1984) *Continental Mesozoic Stratigraphy and Paleontology in Sichuan Basin of China*.  
811 People's Publishing House of Sichuan, Chengdu.
- 812 WIEDENBECK, M., HANCHAR, J.M., PECK, W.H., SYLVESTER, P., VALLEY, J., WHITEHOUSE, M., KRONZ,  
813 A., MORISHITA, Y., NASDALA, L. & FIEBIG, J. (2004) Further characterisation of the 91500 zircon  
814 crystal. *Geostandards and Geoanalytical Research*, **28**, 9-39.
- 815 XIAO, L., ZHANG, H.F., CLEMENS, J.D., WANG, Q.W., KAN, Z.Z., WANG, K.M., NI, P.Z. & LIU, X.M.  
816 (2007) Late Triassic granitoids of the eastern margin of the Tibetan Plateau: Geochronology,  
817 petrogenesis and implications for tectonic evolution. *Lithos*, **96**, 436-452.
- 818 XIE, J., LI, G. & TANG, D. (2006) Analysis on provenance-supply system of Upper Triassic Xujiahe  
819 formation, Sichuan Basin. *Natural Gas Exploration and Development*, **29**, 1-3, 13, in Chinese  
820 with English abstract.
- 821 XIE, T., ZHOU, Z., ZHANG, Q., HU, S., HUANG, J., WEN, W. & CONG, F. (2013) Zircon U-Pb age for the  
822 tuff before the Luoping biota and its geological implication. *Geological Review*, **59**, 159-164, in  
823 Chinese with English abstract.
- 824 XU, X., LIU, B., ZHAO, Y. & LU, Y. (1997) *Sequence Stratigraphy and Basin- Mountain*  
825 *Transformation in the Western Margin of Upper Yangtze Lnadmass during the Permian to*  
826 *Triassic*. Geological Publishing House, Beijing, 1-124pp, in Chinese with English abstract.
- 827 XU, Y., HE, B., CHUNG, S., MENZIES, M.A. & FREY, F.A. (2004) Geologic, geochemical, and  
828 geophysical consequences of plume involvement in the Emeishan flood-basalt province. *Geol*, **32**,  
829 917.
- 830 XU, Z., HOU, L. & WANG, Z. (1992) *Orogenic Processes of the Songpan- Garze Orogenic Belt of*  
831 *China*. Geol. Publ. House, Beijing.

- 832 YAN, D., ZHOU, M., LI, S. & WEI, G. (2011) Structural and geochronological constraints on the  
833 Mesozoic-Cenozoic tectonic evolution of the Longmen Shan thrust belt, eastern Tibetan Plateau.  
834 *Tectonics*, **30**, n/a-n/a.
- 835 YAN, Q., WANG, Z., LIU, S., SHI, Y., LI, Q., YAN, Z., WANG, T., WANG, J., ZHANG, D. & ZHANG, H.  
836 (2006) Eastern Margin of the Tibetan Plateau A Window to Probe the Complex Geological  
837 History from the Proterozoic to the Cenozoic Revealed by SHRIMP Analyses. *Acta Geologica*  
838 *Sinica*, **80**, 1285-1294, in Chinese with English abstract.
- 839 YANG, Z., SHEN, C., RATSCHBACHER, L., ENKELMANN, E., JONCKHEERE, R., WAUSCHKUHN, B. &  
840 DONG, Y. (2017) Sichuan Basin and beyond: Eastward foreland growth of the Tibetan Plateau  
841 from an integration of Late Cretaceous - Cenozoic fission track and (U - Th)/He ages of the  
842 eastern Tibetan Plateau, Qinling, and Daba Shan. *Journal of Geophysical Research Solid Earth*,  
843 **122**, 4712-4740.
- 844 YIN, A. (1996) A Phanerozoic palinspastic reconstruction of China and its neighboring regions, in:  
845 Tectonic Evolution of Asia.
- 846 YUAN, C., ZHOU, M., SUN, M., ZHAO, Y., WILDE, S., LONG, X. & YAN, D. (2010) Triassic granitoids in  
847 the eastern Songpan Ganzi Fold Belt, SW China: Magmatic response to geodynamics of the deep  
848 lithosphere. *Earth and Planetary Science Letters*, **290**, 481-492.
- 849 ZHANG, G.W., MENG, Q.R. & LAI, S.C. (1995) Tectonics and structure of Qinling orogenic belt.  
850 *Science in China*, **38**, 1379-1394.
- 851 ZHANG, H., ZHANG, L., HARRIS, N., JIN, L. & YUAN, H. (2006) U-Pb zircon ages, geochemical and  
852 isotopic compositions of granitoids in Songpan-Garze fold belt, eastern Tibetan Plateau:  
853 constraints on petrogenesis and tectonic evolution of the basement. *Contrib Mineral Petrol*, **152**,  
854 75-88.
- 855 ZHANG, H., PARRISH, R., ZHANG, L., XU, W., YUAN, H., GAO, S. & CROWLEY, Q.G. (2007) A-type  
856 granite and adakitic magmatism association in Songpan-Garze fold belt, eastern Tibetan Plateau:  
857 Implication for lithospheric delamination. *Lithos*, **97**, 323-335.
- 858 ZHANG, Y., TANG, X.D., ZHANG, K., ZENG, L. & GAO, C. (2014) U-Pb and Lu-Hf isotope systematics  
859 of detrital zircons from the Songpan - Ganze Triassic flysch, NE Tibetan Plateau: implications for  
860 provenance and crustal growth. *International Geology Review*, **56**, 29-56.
- 861 ZHANG, L., DING, L., PULLEN, A. & KAPP, P. (2015c) Reply to comment by W. Liu and B. Xia on “Age  
862 and geochemistry of western Hoh-Xil-Songpan-Ganze granitoids, northern Tibet: Implications for  
863 the Mesozoic closure of the Paleo-Tethys ocean”. *Lithos*, **212-215**, 457-461.
- 864 ZHANG, Y., JIA, D., SHEN, L., YIN, H., CHEN, Z., LI, H., LI, Z. & SUN, C. (2015a) Provenance of detrital  
865 zircons in the Late Triassic Sichuan foreland basin: constraints on the evolution of the Qinling  
866 Orogen and Longmen Shan thrust-fold belt in central China. *International Geology Review*, **57**,  
867 1806-1824.
- 868 ZHANG, Y., ZENG, L., LI, Z., WANG, C., ZHANG, K., YANG, W. & GUO, T. (2015b) Late Permian-  
869 Triassic siliciclastic provenance, palaeogeography, and crustal growth of the Songpan terrane,  
870 eastern Tibetan Plateau: evidence from U-Pb ages, trace elements, and Hf isotopes of detrital  
871 zircons. *International Geology Review*, **57**, 159-181.
- 872 ZHAO, J. & ZHOU, M. (2007) Geochemistry of Neoproterozoic mafic intrusions in the Panzhihua  
873 district (Sichuan Province, SW China): Implications for subduction-related metasomatism in the  
874 upper mantle. *Precambrian Research*, **152**, 27-47.
- 875 ZHAO, J., CHEN, Y. & LI, Z. (2006) Zircon U-Pb SHRIMP Dating for the Kangding Complex and Its  
876 Geological Significance. *Geoscience*, **20**, 378-385, in Chinese with English abstract.
- 877 ZHAO, Y., XU, X. & LIU, B. (1996) High-frequency sequences and sea-level oscillations in the Emei  
878 area on the western margin of the Upper Yangtze Platform. *Lithofacies Paleogeography*, **16**, 1-18,  
879 in Chinese with English abstract.
- 880 ZHAO, Z., ZHOU, H., CHEN, X., LIU, Y., ZHANG, Y., LIU, Y. & YANG, Y. (2012) Sequence lithofacies  
881 paleogeography and favorable exploration zones of the Permian in Sichuan Basin and adjacent  
882 areas, China. *Acta Petrolei Sinica*, **33**, 35-51, in Chinese with English abstract.
- 883 ZHENG, Y., LI, H., SUN, Z., WANG, H., ZHANG, J., LI, C. & CAO, Y. (2016) New geochronology  
884 constraints on timing and depth of the ancient earthquakes along the Longmen Shan fault belt,  
885 eastern Tibet. *Tectonics*, **35**, 2781-2806.
- 886 ZHOU, M., MA, Y., YAN, D., XIA, X., ZHAO, J. & SUN, M. (2006a) The Yanbian Terrane (Southern  
887 Sichuan Province, SW China): A Neoproterozoic arc assemblage in the western margin of the  
888 Yangtze Block. *Precambrian Research*, **144**, 19-38.
- 889 ZHOU, M., YAN, D., KENNEDY, A.K., LI, Y. & DING, J. (2002) SHRIMP U-Pb zircon geochronological  
890 and geochemical evidence for Neoproterozoic arc-magmatism along the western margin of the  
891 Yangtze Block, South China. *Earth and Planetary Science Letters*, **196**, 51-67.

892 ZHOU, M., YAN, D., WANG, C., QI, L. & KENNEDY, A. (2006b) Subduction-related origin of the 750  
893 Ma Xuelongbao adakitic complex (Sichuan Province, China): implications for the tectonic setting  
894 of the giant Neoproterozoic magmatic event in South China. *Earth and Planetary Science Letters*,  
895 **248**, 286-300.

896 ZHU, H., ZHOU, B., WANG, S., LUO, M., LIAO, Z. & GUO, Y. (2011) Detrital zircon U-Pb dating by  
897 LA-ICP-MS and its geological significance in western margin of Yangtze terrane. *Journal of*  
898 *Mineralogy and Petrology*, **31**, 70-74, in Chinese with English abstract.

899 ZHU, M., CHEN, H., ZHOU, J. & YANG, S. (2017) Provenance change from the Middle to Late Triassic  
900 of the southwestern Sichuan basin, Southwest China: Constraints from the sedimentary record and  
901 its tectonic significance. *Tectonophysics*, **700-701**, 92-107.

902 ZHU, Z. & WANG, G. (1986) Paleogeography of before and after deposition of green-bean rock (altered  
903 tuff) between the early and middle Triassic in the upper Yangtze platform and its adjacent areas.  
904 *Oil & Gas Geology*, **7**, 344-355, in Chinese with English abstract.

905

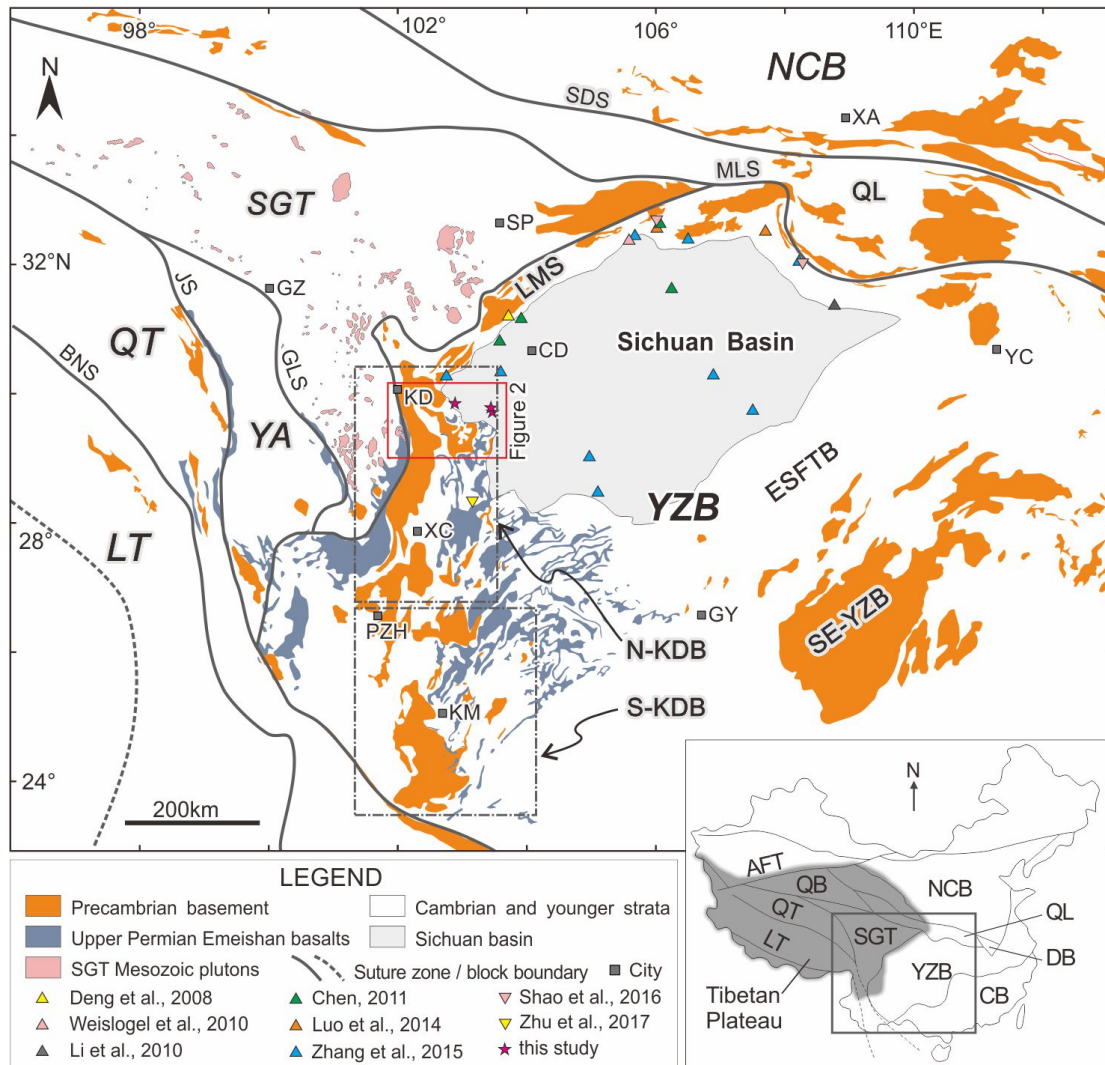
906

907

908

909 Figure captions:

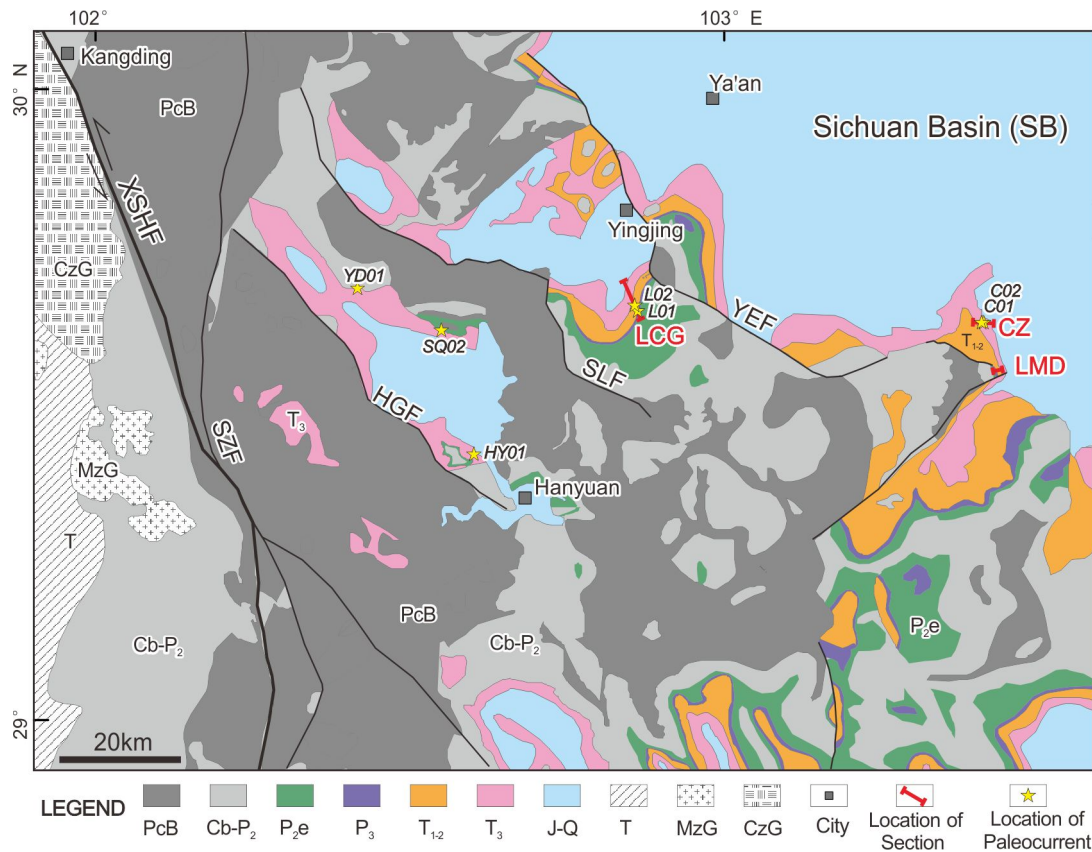
910



911

912 **Fig. 1.** Simplified tectonic map of the upper Yangtze Block and adjacent regions. Sites of previous  
913 detrital zircon geochronology studies of the Sichuan Basin are shown in the figure. Inset shows main  
914 tectonic elements of China. ATF, Altyn Tagh fault; CB, Cathaysia Block; CD, Chengdu; DB, Dabie  
915 orogen; ESFTB, eastern Sichuan fold-and-thrust belt; GLS, Ganze-Litang suture; GY, Guiyang; GZ,  
916 Ganze; JS, Jinshajiang suture; KD, Kangding; KM, Kunming; LMS, Longmen Shan thrust belt; LT,  
917 Lhasa terrane; MLS, Mianlue suture; N-KDB, northern Kangdian basement; NCB, North China Block;  
918 PZH, Panzhihua; QB, Qaidam Block; QL, Qinling orogen; QT, Qiangtang terrane; S-KDB, southern  
919 Kangdian basement; SDS, Shangdan suture; SGT, Songpan-Ganze terrane; SP, Songpan; XA, Xi'an;  
920 XC, Xichang; YC, Yichang; YA, Yidun arc; YZB, Yangtze Block. Modified from Tian *et al.* (2012)  
921 and Wang & Pan, (2013). The distribution of the Upper Permian Emeishan basalts is modified from Xu  
922 *et al.* (2004).

923

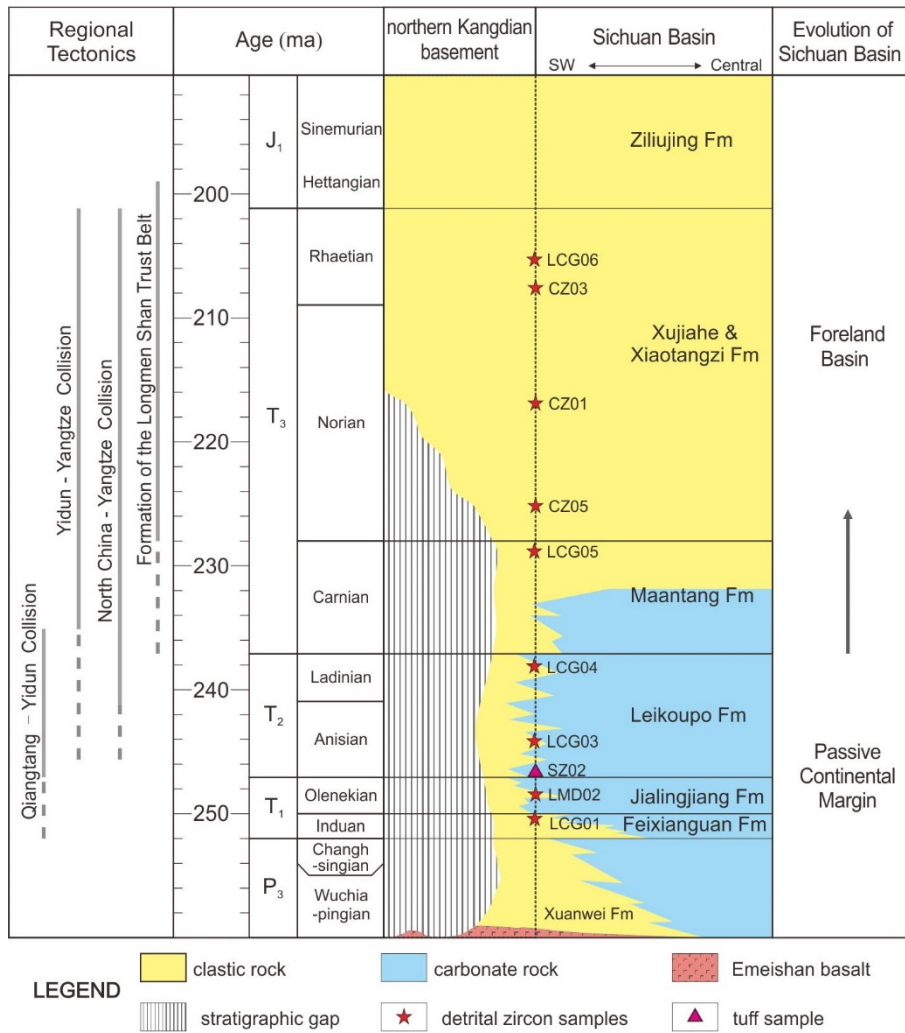


924

925 **Fig. 2.** Generalized geological map of the study area, modified from BGSP (1974). The location of this  
 926 figure is shown in Fig. 1. Abbreviations: Cb-P<sub>2</sub>, Cambrian - Middle Permian; CzG, Cenozoic Granite;  
 927 HGF, Hanyuan-Ganluo fault; J-Q, Jurassic to Quaternary; MzG, Mesozoic Granite; P<sub>2e</sub>, Upper  
 928 Permian Emeishan basalts; P<sub>3</sub>, Upper Permian Xuanwei Formation; PcB, Precambrian basement; SLF,  
 929 Sanhe-Leibo fault; SZF, Shimian-Zhaojue fault; T, Triassic in the eastern Songpan-Ganze terrane; T<sub>1-2</sub>,  
 930 Lower and Middle Triassic; T<sub>3</sub>, Upper Triassic; XSHF, Xianshuihe fault; YEF, Yingjing-Emei fault.  
 931 Red solid lines and text define the localities of the Longcanggou (LCG), Chuanzhu (CZ) and  
 932 Longmendong (LMD) sections, from which samples were collected.

933

934



935

936 **Fig. 3.** Stratigraphic nomenclature, age of the southern Sichuan Basin and northern Kangdian Oldland.

937 The time of formation of the Longmen Shan thrust belt is based on Yin (1996); Meng, et al (2005), Li

938 *et al.* (2003a, 2014); the time of North China – Yangtze collision is after Yin & Nie (1993) Zhang *et*

939 *al.* (1995), Liu *et al.* (2005, 2015); the time of Yidun – Yangtze collision is after Reid *et al.* (2005),

940 Roger *et al.* (2008), Yuan *et al.* (2010), Wang *et al.* (2013a); the time of Qiangtang – Yidun collision

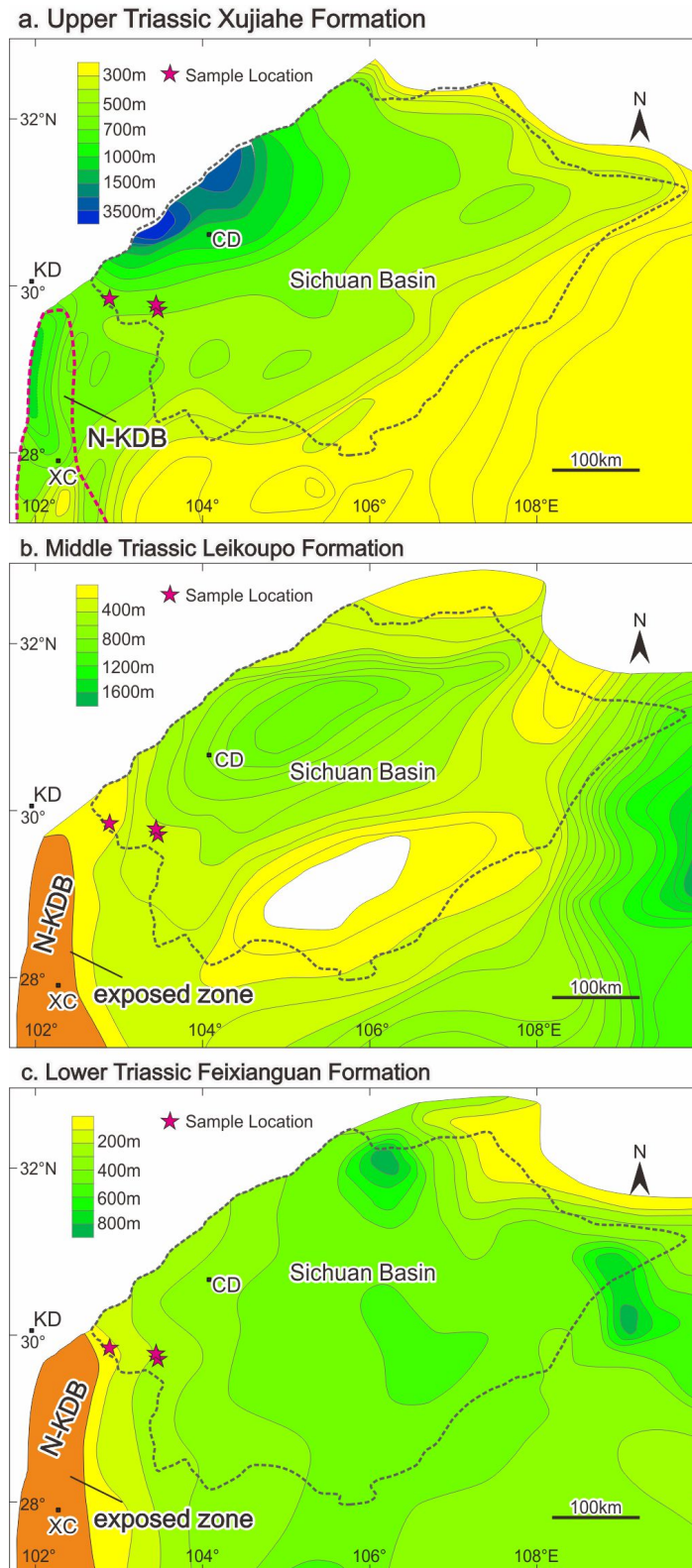
941 is after Reid *et al.* (2005), Pullen *et al.* (2008), Roger *et al.* (2008, 2010). Time scale is from Gradstein

942 *et al.* (2012). J<sub>1</sub>, the Early Jurassic; P<sub>3</sub>, the Late Permian; T<sub>1</sub>, the Early Triassic; T<sub>2</sub>, the Middle Triassic;

943 T<sub>3</sub>, the Late Triassic.

944

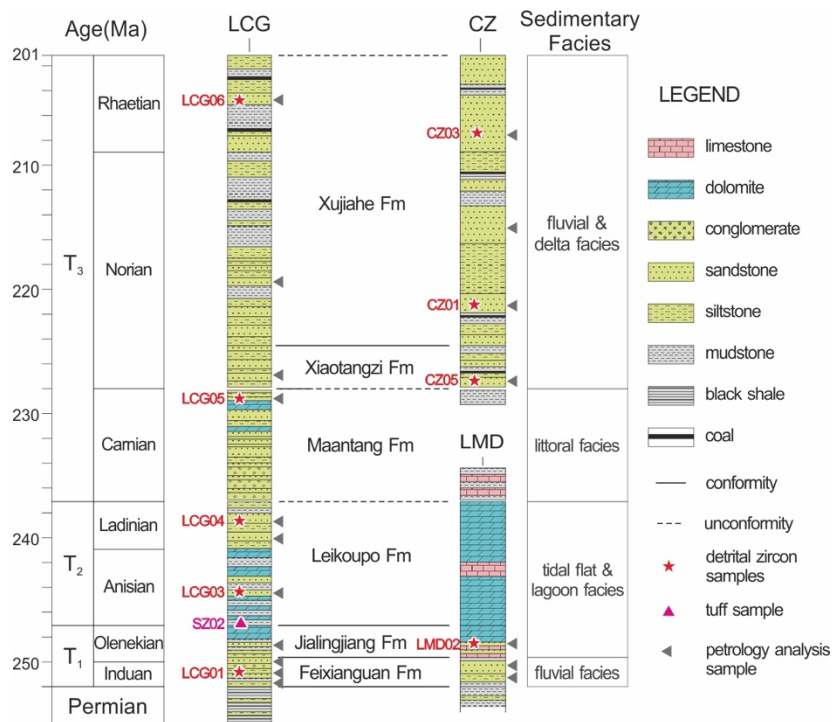




945

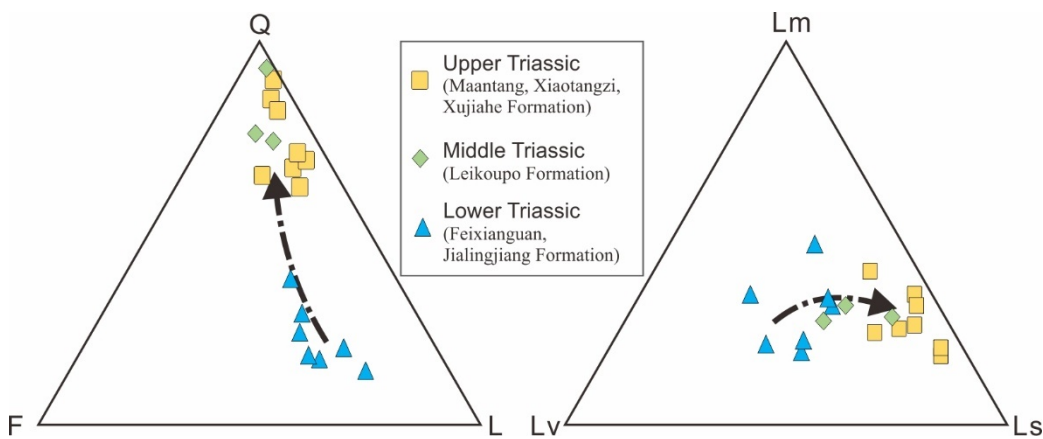
946 **Fig. 4.** Isopach maps of the Late Triassic Xujiahe (a), Middle Triassic Leikoupo (b) and Early Triassic  
 947 Feixianguan (c) Formations in the upper Yangtze Block, including the Sichuan Basin and surrounding  
 948 regions (modified after Guo *et al.* 1996). Note that yellow patches are exposed parts of northern  
 949 Kangdian basement. Abbreviations for towns: CD, Chengdu; KD, Kangding; XC, Xichang. Note that  
 950 in Fig. 4a, the northern Kangdian basement (N-KDB) switched to a depocenter.





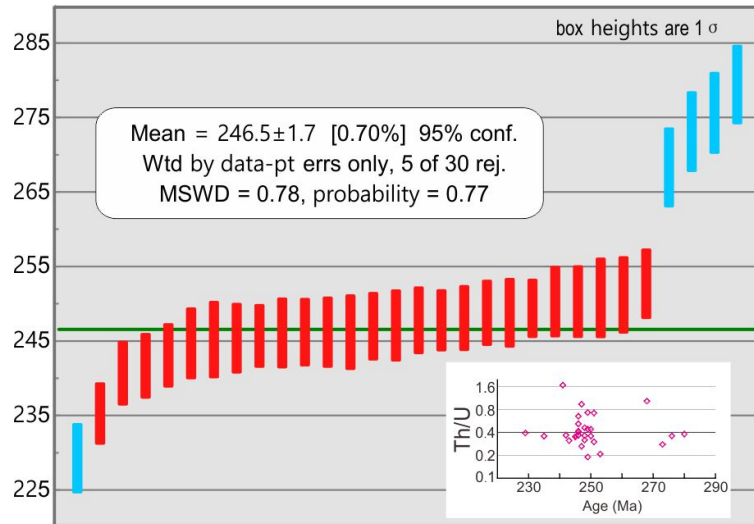
963

964 **Fig. 6.** Comparison of Triassic stratigraphy within the southwestern Sichuan Basin. CZ (Chuanzhu)  
 965 section is compiled from WGCMSPIB (1984) and LMD (Longmendong) section from Lin *et al.*  
 966 (1982), Xu *et al.* (1997) and BGMRSF (1997), with the sedimentary facies after Zhao *et al.* (1996). T<sub>1</sub>,  
 967 T<sub>2</sub> and T<sub>3</sub> are the Early, Middle and Late Triassic, respectively. Time scale is from the Gradstein *et al.*  
 968 (2012), which is consistent with the tuff results derived from the sample SZ02 from the Longcanggou  
 969 (LCG) section (see Fig. 7).  
 970



971

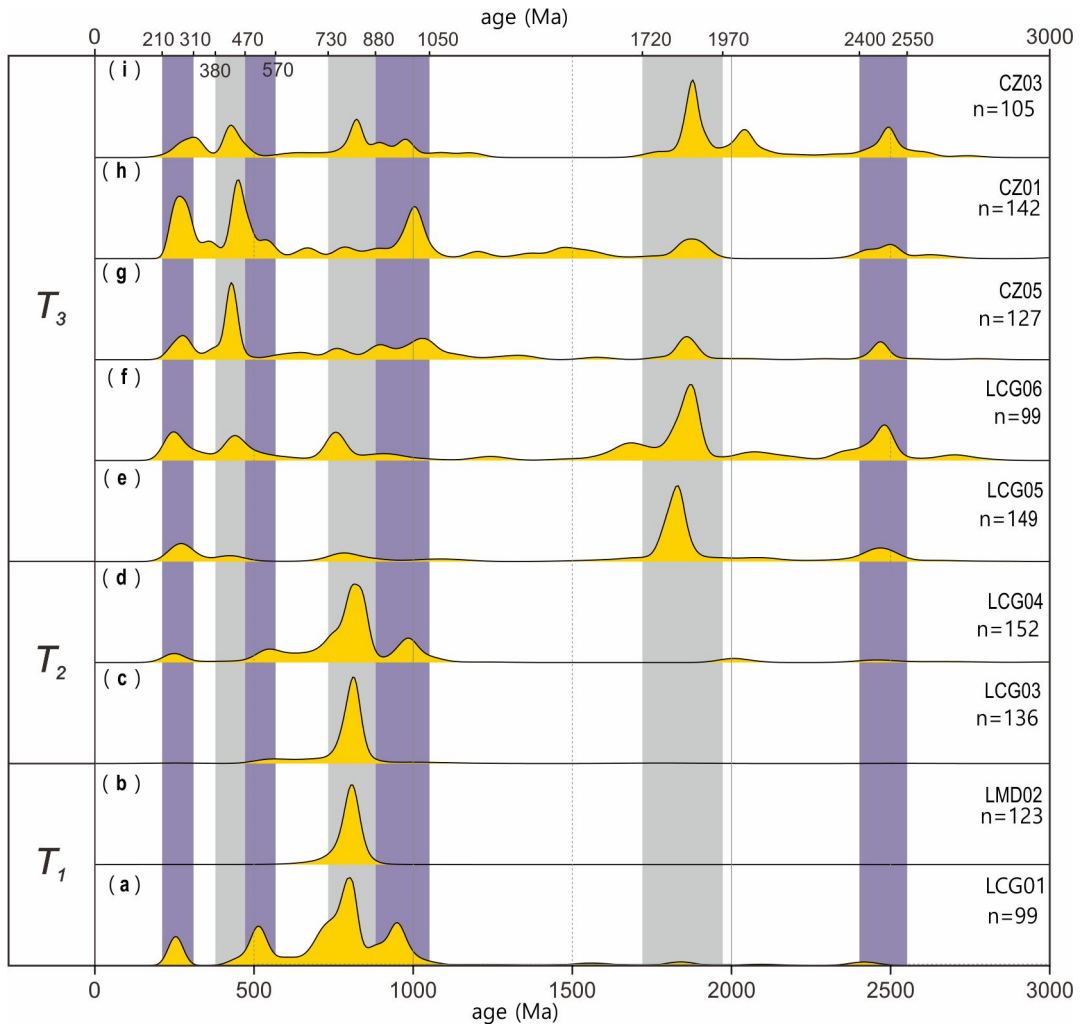
972 Fig. 7. Ternary diagrams for sandstones of the Lower (Feixianguan and Jialingjiang), Middle  
 973 (Leikoupo) and Late Triassic (Maantang, Xiaotangzi and Xujiuhe) formations. Q, quartz; F,  
 974 feldspar; L, lithic fragments (Lm, metamorphic; Ls, sedimentary; Lv, volcanic). The black arrows  
 975 highlight trend of compositional change from lower to upper Triassic deposits.  
 976  
 977



978

979 **Fig. 8.** U–Pb zircon ages from altered tuff sample SZ02. Blue dates are outliers rejected by ISOPLOT  
 980 for calculating the weighted mean age.

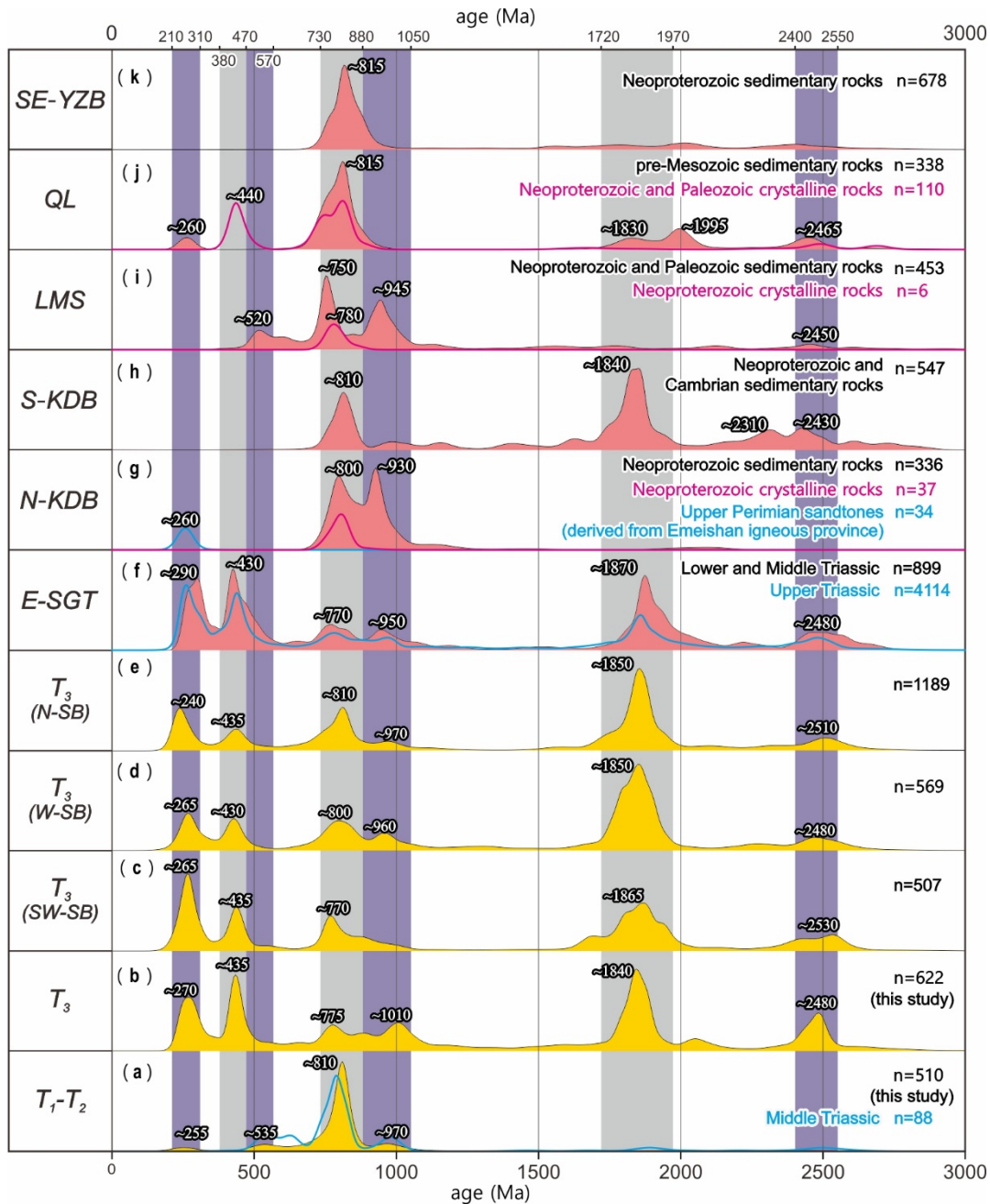
981



982

983 **Fig. 9.** Kernel Density Estimation (KDE) plots of the detrital zircon U-Pb data for samples LCG01,  
 984 LMD02, LCG03, LCG04, LCG05, LCG06, CZ05, CZ01 and CZ03, respectively.

985



987

988 **Fig. 10.** KDE plots of detrital zircon ages from Triassic sediments in the Sichuan Basin and potential  
 989 source areas. (a-b) Age spectra of the Early-Middle and Late Triassic sediments in the southwestern  
 990 Sichuan Basin, Middle Triassic (blue dashline) is after [Zhu, et al., 2017](#). (c-e) Spectra of the Late  
 991 Triassic sediments in the southwestern, western and northern Sichuan Basin, reported in previous  
 992 studies ([Deng et al., 2008](#); [Weislogel et al., 2010](#); [Chen, 2011](#); [Luo et al., 2014](#); [Zhang et al., 2015a](#);  
 993 [Shao et al., 2016](#); [Zhu et al., 2017](#)). Spectra of potential areas, including (f) E-SGT (eastern  
 994 Songpan-Ganze terrane), compiled from the Early-Middle Triassic sedimentary rocks (black solid line)  
 995 ([Weislogel et al., 2006, 2010](#); [Enkelmann, 2007](#); [Ding et al., 2013](#); [Wang et al., 2013a](#)) and the Late  
 996 Triassic sedimentary rocks (blue dash line) ([Wang et al, 2007](#); [Weislogel et al., 2006, 2010](#); [Ding et al.,](#)  
 997 [2013](#); [Wang et al., 2013a](#); [Zhang et al., 2014, 2015b](#)), (g) N-KDB (northern Kangdian Basement),  
 998 compiled from both crystalline (red dash line) ([Roger & Calassou, 1997](#); [Guo et al., 1998](#); [Shen et al.,](#)

999 2000; Li *et al.*, 2001; Li *et al.*, 2002; Zhou *et al.*, 2002; Shen *et al.*, 2003; Li *et al.*, 2003b; Zhou *et al.*,  
1000 2006a; Lin *et al.*, 2006; Yan *et al.*, 2006; Zhao *et al.*, 2006; Geng *et al.*, 2007; Huang *et al.*, 2009; Lin,  
1001 2010; Ruan, 2013; Meng *et al.*, 2015) and sedimentary rocks (black solid line) (Zhou *et al.*, 2006a; He  
1002 *et al.*, 2007; Sun *et al.*, 2009), (h) S-KDB (southern Kangdian Basement), compiled from sedimentary  
1003 rocks (Sun *et al.*, 2009; Wang *et al.*, 2012b), (i) LMS (Longmen Shan thrust belt), compiled from both  
1004 crystalline (red dash line) (Zhou *et al.*, 2006b; Meng *et al.*, 2015) and sedimentary rocks (black solid  
1005 line) (Duan *et al.*, 2011; Chen *et al.*, 2016), (j) QL (Qinling orogen), compiled from both crystalline  
1006 (red dash line) (Li *et al.*, 2016 and references therein) and sedimentary rocks (black solid line) (He *et*  
1007 *al.*, 2007; Wang *et al.*, 2013b), (k) SE-YZB (southeastern Yangtze Block), compiled from sedimentary  
1008 rocks (Wang *et al.*, 2010; Wang & Zhou, 2012).

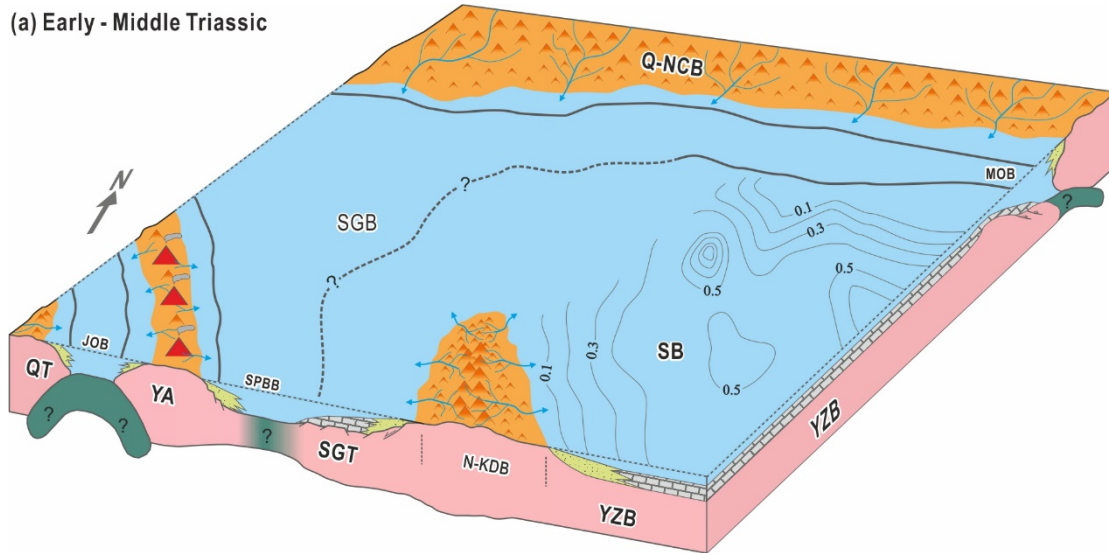
1009

1010

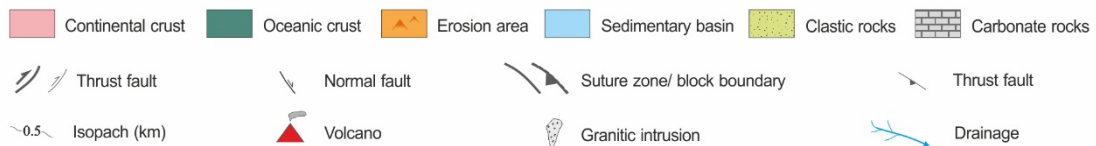
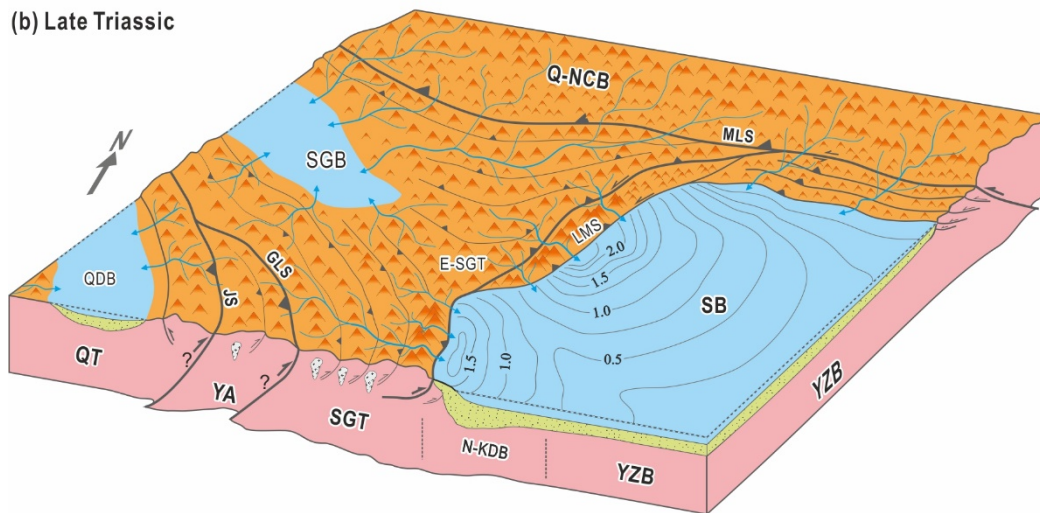
1011

1012

(a) Early - Middle Triassic



(b) Late Triassic



1013

1014

1015

1016

1017

1018

1019

1020

1021

1022

1023

**Fig. 11.** Models for Triassic tectonic evolution of the upper Yangtze Block and its link to adjacent structural belts. E-SGT, eastern Songpan-Ganze terrane; GLS, Ganze-Litang suture; JOB, Jinshajiang Ocean Basin; JS, Jinshajiang suture; LMS, Longmen Shan thrust belt; MLS, Mianlue suture; MOB, Mianlue Ocean Basin; N-KDO, northern Kangdian basement; QDB, Qamdo Basin; Q-NCB, Qingling Terrane and North China Block; QT, Qiangtang terrane; SB, Sichuan Basin; SGB, Songpan-Ganze Basin; SGT, Songpan-Ganze terrane; SPBB, Songpan back arc Basin; YA, Yidun arc; YZB, Yangtze Block. The tectonic evolution between Qiangtang terrane and northern Kangdian basement is after Roger *et al.* (2008)